UNIVERSITY OF TURIN

Department of oncology

School of Life and Health Sciences
Doctorate in Molecular Medicine
Cycle XXXIII
Academic years 2017-2021

The interplay between DNA damage response pathways and chemotherapy resistance in metastatic colorectal cancer

Tutor
Prof. Andrea Bertotti

PhD candidate
Marco Avolio

Coordinator
Prof. Francesco Novelli

TABLE OF CONTENT

ABSTRACT

The standard-of-care treatment for patients with metastatic colorectal cancer (mCRC) includes a backbone of cytotoxic agents, namely 5-fluorouracil in combination with irinotecan (FOLFIRI) or oxaliplatin (FOLFOX). Despite the improvement in the management of the disease, mCRC shows a poor 5-year overall survival. A significant contribution to mCRC dismal prognosis is given by the paucity of information about the mechanisms underlying chemoresistance and lack of molecularly-based patient stratification. Here, we investigated the emerging role of DNA damage response (DDR) as a putative modulator of chemotherapy sensitivity in mCRC and sought to find response predictors of potential clinical use.

By employing a large panel of patient-derived xenograft (PDX) models, we demonstrated that this platform faithfully captured the divergence between FOLFIRI-resistant and sensitive mCRCs observed in patients. By integrating experimentation in matched PDXs and organoids, we identified proficiency of the homologous recombination (HR) pathway as a candidate mechanism of FOLFIRI resistance; consistent with proper HR functionality, refractory models i) accumulated less double-strand breaks after FOLFIRI; ii) were less susceptible to PARP blockade than responsive tumors; iii) exhibited higher basal levels of RAD51, a critical upstream regulator of the HR pathway, and higher treatment-induced RAD51 activity. Importantly, RAD51 expression could be easily assessed by routine immunohistochemistry tests with diagnostic portability.

The influence of DDR on response to chemotherapy is supported by the observation that FOLFIRI-resistant tumors were enriched for mutations of *ATR*, a key sensor of DNA replication stress. We found that tumors harboring heterozygous *ATR* mutations were particularly sensitive to ATR blockade, likely because they were more reliant on hypomorphic ATR function and RAD51 activity for rescuing stalled replication forks and progress through the cell cycle.

Collectively, our results illustrate the impact of HR-mediated DNA repair on the outcome of genotoxic therapy in mCRC and put forward RAD51 as a potential biomarker of resistance to FOLFIRI, which could be exploited in the clinic to improve therapeutic decision making.

INTRODUCTION

THE DNA DAMAGE AND THE DNA DAMAGE RESPONSE PATHWAYS

Inducers and types of DNA damages

In all living organisms, the genetic information is faithfully delivered to the next generations thanks to the DNA double-helical structure [1], which is constantly perturbed by lesions procured by exogenous and endogenous stimuli [2]. Exogenous DNA damages are produced by both physical and chemical agents, and their relationship with genetic changes and cancer promotion were already understood before the discovery of the double helix in 1953[3]. Ionizing radiation (IR) and ultraviolet (UV) light from sunlight can induce pyrimidine dimers and 6–4 photoproducts. IRs are also able to generate single-strand breaks (SSBs), and the most toxic DNA damage double-strand breaks (DSBs), by DNA base oxidation. Cancer-causing DNA-damaging chemicals are numerous and include tobacco smoke, dietary carcinogens, such as heterocyclic amines, and other chemicals whose production is the consequence of exposure principally to arsenic, air pollution, aflatoxin, polychlorinated biphenyls, radon, asbestos. Furthermore, agents used to treat cancer also cause DNA lesions: alkylating agents, such as temozolomide, are responsible for DNA methylation; topoisomerase I and II inhibitors induce SSBs or DSBs; crosslinking agents, such as cisplatin, are able to induce intra- and, mainly, inter-strand crosslinks between DNA bases [4].

Besides exogenous insults, DNA aberrations also occur endogenously through physiological processes in the human body. DNA mismatches naturally arise during DNA replication; DNA strand breaks are the consequences of the flawed activity of topoisomerase enzymes, whereas DNA-base lesions are often generated by hydrolytic reactions and non-enzymatic methylations. Moreover, reactive oxygen species (ROS) and nitrogen compounds, derived from the physiological cellular metabolism, contribute to the DNA lesions by causing erroneous base

pairing, base loss, base oxidation, DNA SSBs and block of DNA replication and transcription [2]. Altogether, these spontaneous damages affect the DNA molecules around 10^5 per cell daily [5].

The DNA damage response pathways

To maintain genomic integrity and prevent incorrect transmission of genetic information to the progeny, DNA must be protected from the numerous lesions occurring daily. Thus, cells have evolved an elaborate network, termed DNA-damage response (DDR), to detect lesions, signal their presence and promote their repair (**Figure 1**) [6].

Repair pathway	NHEJ	HR	alt-NHEJ/ MMEJ	SSA	ICL repair	SSB repair	BER	TLS	NER	MMR
Source of DNA damage	IR, radiomimetics, Topo II inhibitors	X-linking agents, replication inhibitors, antimetabolites, Topo I inhibitors			X-linking agents	IR, ROS, radiomimetics Topo I inhibitors H_2O_2, alkylating agents	Alkylating agents	UV, alkylating agents	Alkylating agents, X-linkers	DNA Pol proofreading errors
Damage sensors	Ku70/Ku80	MRN	PARP	MRN	FA core complex (FANCA, B, C, E, F, G, L and M)	PARP	DNA glycosylases, APE1	PCNA	XPC DDB2 CSA	MSH2, MSH3, MSH6, MLH1, PMS2
Signaling/ mediator proteins	DNAPK	ATM, ATR, MK2, CtIP, BRCA1/BARD1, BRCA2, PALB2, RPA		CtIP	FANCD1 [BRCA2] D2, I J [BRIP1] N [PALB2] O [RAD51C] P [SLX4]			RAD6 RAD18	XPA, XPF RPA	
Effector proteins	XRCC4 XLF LIG4 APLF Artemis PAXX WRN	RAD51 MUS81/EME1 SLX1/SLX4 RTEL1 BLM TOPOIII POLQ PARI RECQL5 FANCJ, BLM	XRCC1 LIG3, LIG1 CtIP POLQ	RAD52, others?	Shared with HR, TLS, and NER	XRCC1 PNKP POLβ FEN1, TDP1 Aprataxin, LIG1, LIG3A	As for SSB repair	REV1, POLH POLI, POLK	XPG ERCC1 POLE POLD1 LIG1, LIG3	EXO1 POLD LIG1

Figure 1. Principal repair mechanisms of DNA damage. Illustration of the main molecular pathways involved in DNA damage repair along with representative targets for which drugs have been developed (in red). Each signaling pathway consist of sensors, mediators and effector proteins able to recognize and repair the different types of DNA lesions. Adapted from Brown JS et al., Cancer Discov., 2017.

The machinery consists of several molecular pathways, specific for each DNA lesion, operating in different phases of the cell cycle and closely linked with replication, transcription, recombination, chromatin remodeling and differentiation [4, 7]. Although distinct, the pathways are functionally interwoven and operate to ensure cell survival or, in case of irreparably damage, to induce replicative senescence or death. Irreversible exit from the cell cycle (senescence) or apoptosis (programmed cell death) are inherent safeguard mechanisms to avoid genomic instability, which fuels cancer onset and progression by increasing genetic diversity and thus by favoring the emergence of fitter variants [8].

O^6-methylguanine DNA methyltransferase (MGMT)

The simpler mechanism of DNA repair relies on the direct activity of proteins, such as O^6-methylguanine DNA methyltransferase (MGMT). MGMT is a DNA "suicide" repair enzyme, able to repair O^6-methylguanine lesions (O^6-meG) induced by methylating agents, by transferring the alkyl group from the O^6-position of guanine to a cysteine residue within its active site pocket. Once the guanine is restored, the alkylated MGMT is thus ubiquitinated and degraded by the proteasomal system [9].

Nucleotide excision repair

The nucleotide excision repair (NER) pathway is involved in restoring different lesions that disrupt the helical structure of the DNA. Main examples are: the pyrimidine dimers and 6–4 photoproducts produced by UV radiation, and the base adducts derived from exogenous agents, such as cisplatin, which hinder the progression of polymerases (DNA-pol or RNA-pol), resulting in replication fork collapse or stalled transcription [9]. To remove these adducts, cells use two different pathways, global genome repair NER (GG-NER) and transcription-coupled NER (TC-NER). These pathways exploit common proteins but act on different sites of the genome. In

particular, TC-NER operates on lesions in the transcribed strand of an active gene, whereas GG-NER repairs damages located throughout the genome (transcribed and untranscribed DNA strands, in active and inactive genes), in a cell cycle-independent manner [7]. Following the identification of the lesion by xeroderma pigmentosum complementation group C (XPC), the two nucleases XPF-ERCC1 and XPG trigger the removal of the 22-30-base damage oligonucleotide – a key aspect of NER. A single strand DNA (ssDNA) is generated; then, DNA polymerases δ, ε or κ carry out the synthesis of the new oligonucleotide, whereas ligases (LIG1, LIG3) seal the nick.

Base excision repair

When DNA bases are modified by oxidation, deamination or alkylation, induced by UV, IR or ROS, the base excision repair (BER) pathway is activated to repair lesions and prevent the detrimental consequences of these DNA modifications. For example, oxidation of guanine generates 8-oxo-dG, one of the most abundant lesions affecting DNA, which is highly mutagenic as it can pair with adenine (or cytosine) during DNA replication and cause G:C to T:A transversion mutations [9]. To remove such lesion, BER employs several proteins, mainly glycosylases, which are able to recognize and remove the impaired base. This excision creates an abasic site that is subsequently processed by apurinic/apyrimidinic endonuclease 1 (APE1). As a result, 3'-OH and 5'-P termini are generated and consequentially resolved through either the short-patch (SP or single-nucleotide) pathway, which engages DNA-pol β to replace the missing nucleotide, or through the long-patch (LP) pathway, employing DNA-pol δ or ε. The repair is supposed to occur mainly in the G1 phase of cell cycle, before DNA replication, and it is strictly intermingled with the molecular events needed to repair the single-strand breaks [6, 7, 9].

Mismatch repair

The mismatch repair (MMR) system represents one of the most important guardians of genome integrity and it has been preserved from bacteria to humans [10]. MMR proficiency is required for the detection and replacement of base-base mismatches and it is essential for correcting small insertions and deletions - insertion/deletion loops (IDLs) - that occur across repetitive sequences, named microsatellites, along the newly synthesized DNA strand. Deficiency of MMR leads to persistent IDLs, resulting in a mutator phenotype (elevated spontaneous mutation rate) that is accompanied by microsatellite instability (MSI) and cancer [11].

In mammalians, the repair of DNA mismatches employs molecular complexes consisting of seven different proteins, namely MLH1, MLH3, MSH2, MSH3, MSH6, PMS1, and PMS2. The dominant mismatch-binding factor is composed of MSH2 and MSH6, referred as MutSα, which initiates the repair of base-base mismatches and IDLs of one or two extrahelical nucleotides [12, 13], whereas the repair of larger IDLs (more than 2 nucleotides) is initiated by MutSβ, which is a MSH2 and MSH3 heterodimer. MutL heterodimers are also present, consisting of MutLα (MLH1 and PMS2), MutLβ (MLH1 and MLH3), and MutLγ (MLH1 and PMS1), and their functions overlap in substrate specificity with MutS complexes [10]. Once MutS is bound to DNA, MutL heterodimers (mainly MutLα) are recognized, and other proteins, such as proliferating cell nuclear antigen (PCNA), are recruited to the site of DNA damage. Subsequently, EXO1 is recruited, which catalyzes the 5′→3′ degradation of the mismatch from the nascent strand. The gap is filled by DNA-pol δ or ε (with proofreading activity) and sealed by LIG1 [11].

DNA single strand break repair

It has been estimated that DNA single-strand breaks occur tens of thousands times per cell per day, thus representing one of the most common lesions in DNA [5]. This kind of damage can arise as a consequence of different type of stimuli, such as oxidative stress generated by

endogenous ROS (for example H_2O_2), disintegration of the oxidized DNA sugars or base oxidation and abasic site creation promoted by BER. Moreover, abortive activity of enzymes like DNA topoisomerase I (Top I) can lead to SSB, as it creates a temporary lesion needed to relax DNA during transcription and DNA replication [14]. Unrepaired SSB impacts on the cell fate in different manners, but the major consequence is the blockage or the collapse of DNA replication forks during chromosome duplication, leading to the deleterious formation of DSBs. Although cells can resolve DSBs, high cellular levels of SSBs can saturate the pathway, causing persistent SSBs and DSBs that in turn generate genomic instability. To combat these threats, cells are equipped with numerous proteins able to detect the SSB, process the DNA ends, fill the gap, and seal the nick. This enzymatic cascade operates throughout the genome and the cell cycle – but mainly in S phase [7, 14] – and begins thanks to poly (ADP-ribose) polymerase-1 (PARP1) protein, a master sensor of SSB damage [15]. PARP1 binds the DNA break and activates by poly-ADP rybosilation (PARylation) itself and other proteins, such as X-ray repair cross-complementing protein 1 (XRCC1), which serves as a molecular scaffold for other components necessary for the repair. Successively, the 3′- and/or 5′-termini generated by PARP1 activity are processed by specific proteins that are engaged depending on the type of damaged termini. For instance, 5'-deoxyribose phosphates (5′-dRPs), created upon the cleavage of abasic sites by APE1 during BER, are removed by DNA-pol β, whereas 3′-phosphate and 3′-phosphoglycolate termini are processed by polynucleotide kinase/phosphatase (PNKP), APE1, flap endonuclease-1 (FEN-1), tyrosyl DNA phosphodiesterase 1 (TDP1) and aprataxin (APTX). The subsequent gap filling occurs mainly thanks to DNA-pol β, although DNA-pol δ or ε can conduct the process, whereas the final step of ligation is carried out by ligase 1 and ligase 3A (LIG1, LIG4A) [16, 17].

Double-strand break repair

When the lesion affects both DNA strands, a DSB occurs. This lesion is one of the most toxic and difficult to repair [6] and, if not properly fixed, strongly promotes genome instability. DSBs arise

either endogenously, through the activity of ROS, or by exposure to exogenous sources, such as IR or chemotherapeutic agents, among others topoisomerase I and II inhibitors. To avoid harmful consequences, cells exploit two different molecular pathways to contrast the lesion: the homologous recombination (HR) pathway and nonhomologous and joining (NHEJ) pathway (**Figure 2**). The choice between the two molecular events depends on the phase of the cell cycle and the nature of DSB ends [18].

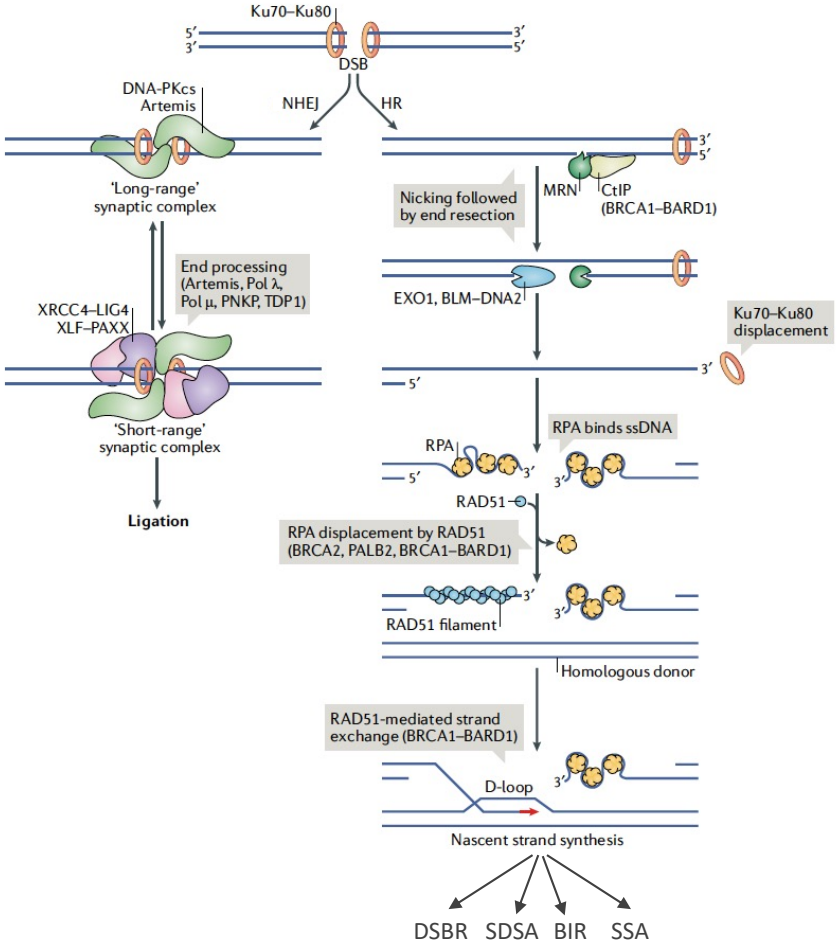

Figure 2. Double-strand break repair pathways. Double-strand breaks are resolved by non-homologous end joining (NHEJ) or homologous recombination (HR) pathways, depending on the phase of the cell cycle and the nature of DSB ends. HR operates in the S and G2 phases of the cell cycle, and 5'-3' DNA resection is the key step that triggers the process. After resection operated by the MRN complex along with CtIP, EXO1, BLM, DNA DNA2 and BRCA1-BARD1, the 3' single- stranded DNA generated is coated by the RPA protein, which is rapidly displaced by RAD51 to form the nucleoprotein filament. Acting in concert with BRCA2, PALB2 and BARD1, the RAD51-filament invades the donor DNA template and creates a D-loop structure that is resolved by different subpathways, depending on the nature of the recombination synapse (see Figure 3). Conversely, NHEJ operates throughout the cell cycle; the process is triggered by the Ku70/Ku80 heterodimer that binds to DSB ends, and in collaboration with DNA-PKs stabilizes and prevents the DNA ends resections. Afterwards, Artemis reveals complementary nucleotide and DNA-pol μ and λ fill the gap. Adapted from Scully R., Nat Rev Mol Cell Bio, 2019.

Homologous recombination

HR operates in the S and G2 phases of the cell cycle, as it requires a homologous sister chromatid for execution. Phosphorylation of the histone variant H2AX (γ-H2AX) is one of the first events that occurs immediately after DSB formation and it is mandatory for the accumulation of other DNA repair proteins around the DSB site [19]. Among the recruited proteins breast cancer type 1 susceptibility (BRCA1) participates, in complex with BRCA1-associated RING domain protein 1 (BARD1), to 5'-3' resection of DNA ends. The 5'-3' DNA resection is the key step of the process and commits cells to employ HR to repair the DSBs, preventing the repair by NHEJ. The first factor recruited to the lesion is the Mre11-Rad50-Nbs1 (MRN) complex that directly binds to double-stranded DNA (dsDNA) and rapidly recruits the master transducer ataxia-telangiectasia mutated (ATM), along with ATM- and Rad3-Related (ATR) and DNA-dependent protein kinase (DNA-PKcs), which are all member of the phosphatidylinositol-3-kinase-like (PIKKs) kinase family [20].

ATM triggers a cascade of events through the interaction with the mediator of DNA damage checkpoint protein-1 (MDC1). In particular, ATM phosphorylates checkpoint kinase 2 (CHK2), which in turns phosphorylates numerous substrates involved in DNA repair, cell cycle regulation, p53 signaling, and apoptosis. For example, CHK2 phosphorylates the cell division cycle 25 A (Cdc25A) phosphatase, preventing the dephosphorylation and activation of cyclin-dependent kinase 2 (Cdk2), thus controlling the intra S checkpoint, arresting the cycle in the S phase [21]. Further, CHK2 phosphorylates p53, with the ensuing upregulation of p21 expression, p21-dependent inhibition of Cdk4/6 activity, and cell-cycle arrest in G1 phase [22]. Activation of p53 may also lead to either apoptosis, through the transcriptional induction of pro-apoptotic components along the extrinsic and intrinsic pathways, or senescence [23]. Instead, the G2/M arrest occurs upon CHK2-mediated phosphorylation of Cdc25C, which results in Cdc25C translocation to the cytoplasm through an interaction with 14-3-3 protein; when

compartmentalized in the cytoplasm, Cdc25C is prevented from activating the cyclin B1/Cdk1 complex, which is necessary for the G2/M transition [24].

Once the lesion is sensed by ATM, BRCA1 recruits partner and localizer of BRCA2 (PALB2), which serves as a molecular scaffold for the engagement of breast cancer type 2 susceptibility (BRCA2) protein. BRCA2 assembles RAD51 onto the 3' ssDNA and disassembles the replication protein A (RPA), a heterotrimeric complex (RPA1, RPA2, RPA3) that typically coats ssDNA, with the help of RAD51 paralogs (RAD51B, C, D, XRCC2/3) [25]. BRCA2 helps RAD51 to nucleate, elongate and stabilize the filament, then RAD51-ssDNA strand searches for a homologous sequence by invading the donor dsDNA, forming a joint molecule with a displaced strand (D loop) [26]. The free 3'-end of the invading strand is extended by DNA polymerases (mainly DNA-pol δ) to reestablish the missing sequence. The final repair can occur by different models depending on the fate of the RAD51-mediate synapse (**Figure 3**).

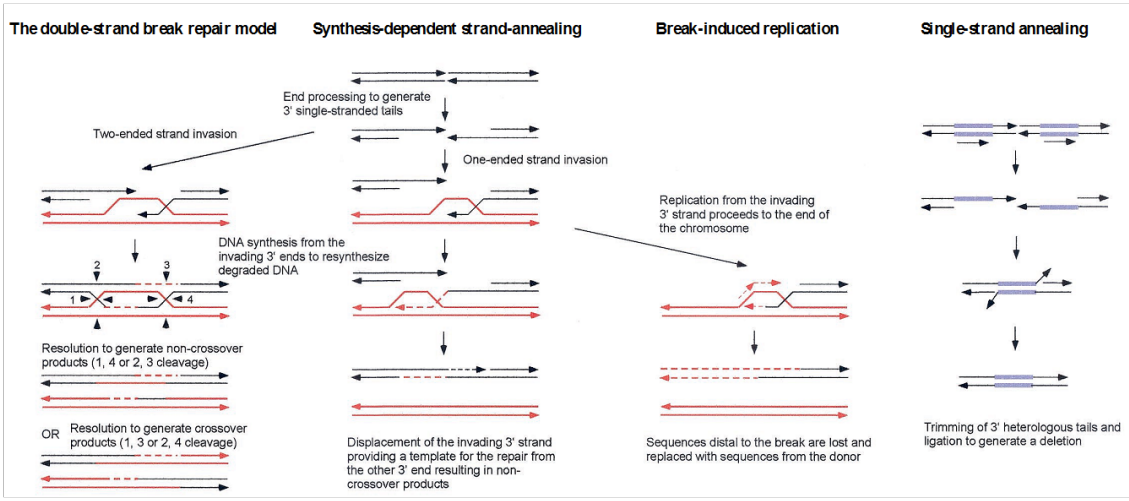

Figure 3. Models for resolutions of DSBs. In the double-strand break repair (DSBR) model, the double Holliday junction intermediate can be resolved by endonucleolytic cleavage of the two Holliday junctions to generate crossover or non-crossover products. In synthesis-dependent strand-annealing (SDSA), the nascent DNA strand pairs with the other 3' single-stranded tail and DNA synthesis completes the repair. The initial phases of the break-induced replication (BIR) mechanism are similar to SDSA, but in this case the 3' DNA strand is extended to the end of the DNA molecule, resulting vulnerable to mutations and rearrangements. In the single-strand annealing (SSA) model, two extensive homologous 3' ssDNA ends are resected extensively to reveal complementary sequences. Afterwards, the single-stranded DNA anneals, resulting in large sequence deletions. Adapted from Symington LS., Microbiol Mol Bio Rev., 2002

DSBs activate not only ATM, but also ATR through ATR interacting protein (ATRIP). Unlike ATM, ATR is not limited to sensing DSBs and responds to many types of genotoxic stress, including stress induced by UV, DNA polymerase inhibitors, deoxyribonucleoside triphosphate depletion, topoisomerase poisons, base-alkylating agents, and DNA crosslinkers. The consequence common to all such perturbations of is the induction of replication stress, which stalls replication fork progression [27]. The ATR-ATRIP complex congregates to the lesion upon the resection of 5′ DNA either side of the DSB. The recruitment is operated by the MRN complex along with CtBP-interacting protein (CtIP), exonuclease 1 (EXO1), Bloom syndrome (BLM) helicase, DNA replication ATP-dependent helicase/nuclease 2 (DNA2) and BRCA1-BARD1, with the final aim to generate a long 3' single-stranded DNA tail, the key structure for ATR activation in response to DSBs [19, 28]. ssDNAs are rapidly coated by RPA, which recruits the ATR-ATRIP complex. At this step, ATR-ATRIP complex recruits RAD17-Rfc2, loads the 9-1-1 complex (RAD9–RAD1–HUS1) at the damaged DNA, and interacts with RAD9, topoisomerase II binding protein (TopBP1) and RAD9–HUS1–RAD1-interacting nuclear orphan (RHINO). TopBP1 is essential for full activation of ATR, which now triggers a cascade of signals that arrest the cell in S or G2/M phase by phosphorylating checkpoint kinase 1 (CHK1). During this block, ATR-dependent signals promote replication fork stabilization, suppress origin firing and stimulate fork repair and restart [27].

The DSB repair model is a canonical HR pathway, abundant in meiotic cells and characterized by the presence of double Holliday junctions (quaternary structures created between two homologous DNA molecules), whose resolution generates either cross-over or non- cross-over products. Alternatively, the synthesis-dependent strand-annealing (SDSA) is the major pathway used by somatic cells. SDSA does not involve Holliday junction formation, therefore it is a non-crossover pathway. A third model, named break-induced replication (BIR), is an alternative

pathway, highly mutagenic and activated when DSBs are single-ended. In this case, DNA synthesis generates extensive 3' ssDNAs that are vulnerable to mutations and rearrangements. This model frequently occurs at telomeres or at broken replication forks. Similarly, the single-strand annealing (SSA) model joins two extensive homologous 3' ssDNA ends without involving sister chromatid exchange. This pathway is important to repair genomes that contain many repeated sequences. In this context the annealing occurs only when resection is sufficient to reveal complementary single-stranded regions, a process that generates large sequence deletions. [26, 29, 30].

Non-homologous end joining

The NHEJ pathway is the major DSB repair mechanism and it operates throughout the cell cycle, as the mechanism does not require a homologous sister chromatid. Indeed, factors that promote DNA resection that commits cells to employ HR are more active during S and G2 phases and less in G1, where the NHEJ primarily occurs. Vice versa, during the cell cycle, and mainly in G1 phase, the tumor suppressor p53-binding protein 1 (53BP1) and the shieldin complex, made up of the SHLD1, SHLD2, SHLD3, and REV7 proteins, block the end resection, preventing the formation of a ssDNA 3′ overhang and the HR cascade [9, 30, 31]. In mammalian cells, NHEJ is sustained by two alternative mechanisms: classical-NHEJ (c-NHEJ) and alternative end joining (aEJ).

c-NHEJ is triggered thanks to the Ku70/Ku80 heterodimer that binds to DSB ends. Ku70/Ku80 recruits other c-NHEJ factors, such as the DNA-dependent protein kinase catalytic subunit (DNA-PKcs), allowing the stabilization and the alignment of the DNA ends. Afterwards, other components are recruited, namely the DNA ligase IV (LIG4), the associated scaffolding factors XRCC4, XRCC4-like factor (XLF), the paralogue of XRCC4, XLF (PAXX) and Artemis, which trims the 3' and 5' single-stranded overhangs at the DNA ends to reveal complementary

nucleotide stretches [30]. After the remotion of existing 3′-P groups or addition of 5′-P residues, DNA-pol μ and λ fill the gap, and the complex formed by XLF, XRCC4 and LIG4 stimulates the end joining. As the ligation of the DNA ends may occur between different chromosomes, the c-NHEJ leads to deletions and translocations [32].

On the contrary, aEJ occurs on 3′ ssDNA ends and, differently from c-NHEJ, it does not depend on c-NHEJ factors. aEJ involves limited displacement of RPA from ssDNA, which reveals microhomology (MH) between strands and facilitates repair [33]. Moreover, aEJ utilizes proteins used also in HR or SSBR, such as the MRN complex, PARP-1, WRN and LIG1, whereas DNA synthesis is exclusively carried out by DNA-pol θ [34]. The complete molecular cascade of aEJ is not fully understood, but it seems that the pathway is more error-prone than c-NHEJ, thus leading to significant genomic instability [9].

Interstrand crosslink repair

Interstrand crosslinks (ICLs) are highly toxic DNA lesions that inhibit the separation of the two strands of the DNA double helix, an essential step for DNA replication and transcription. Exogenous sources that prevalently lead to ICLs are represented by chemotherapeutics agents, such as platinum compounds (cisplatin, carboplatin, oxaliplatin), nitrogen mustards (such as melphalan), psoralen and mitomycin C [35]. ICLs are also generated by endogenous compounds, like metabolites of alcohol, cigarette smoke products and dietary fat [36]. Thus, understanding how cells repair such kind of lesions is of pivotal importance to explore the mechanisms underlying chemotherapy resistance in cancer. To this effort, the Fanconi anemia (FA) disorder has allowed to get insight into the question, as the FA pathway has the primary function of resolving ICLs [37]. This pathway, which mainly operates during the S phase of the cell cycle, involves the coordination of several repair systems, including HR, NER and (discussed below) translesion synthesis [38-40].

The molecular cascade starts when ICLs are recognized by UHRF1 along with the FANCM–MHF1–MHF2 complex, with the ensuing recruitment of the FA complex (composed of 14 proteins: FANCA, FANCB, FANCC, FANCE, FANCF, FANCG, FANCL, FANCM, FANCT, FAAP100, MHF1, MHF2, FAAP20 and FAAP24) to chromatin. The FA complex monoubiquitylates FANCD2-FANCI, stabilizing their interaction with damages sites. This step is necessary for the recruitments of SLX4/FANC, which serve as scaffolds for the DNA endonucleases MUS81, SLX1 and XPF/ERCC4/FANCQ. These endonucleases cleave the DNA strand contiguous to the ICL, generating a DNA adduct and an ICL-derived DSB. The adduct is bypassed by polymerases of the translesion synthesis complex, while DSB is resected by the DNA exonucleases CtIP, MRN and EXO1, thereby generating a 3' single-stranded DNA overhang that is coated by RPA. Subsequently, BRCA1 and BRCA2 initiate HR, in concomitance with the activation of RPA-ATR-CHK1 signaling that slows down DNA replication, allowing the repair [35, 37]. Hence, nucleases from NER make the incisions, translesion synthesis polymerases fill the gap, and finally HR resolves the damage.

Translesion synthesis and template switching mechanisms

Replication block represents a threat that needs to be overcome to maintain genomic stability. Thus, cells have evolved two mechanisms that promote DNA damage tolerance in S phase, allowing to bypass the ssDNA lesion, leaving the damage to be repaired later [41]. The first mechanism is translesion synthesis (TLS), in which conventional DNA polymerases are temporarily replaced by a translesion DNA polymerase (consisting of four Y-family polymerases, pol η, pol ι, pol κ and REV1, one B-family polymerase, pol ζ, and two A-family polymerases pol θ and pol ν), which fills the gap [42]. The mechanism is error-prone, as translesion DNA polymerases lack the proofreading activity and may encourage incorporation of wrong nucleotides.

The other model, template switching (TS), is an error-free pathway as the nascent DNA strand switches to the newly synthesized undamaged sister strand, allowing the replication over the lesion. The pathways share similarities with HR, and the critical step that commits cell to employs TS or TLS is the ubiquitination of the PCNA protein. In mammals, mono-ubiquitination of PCNA, carried out by RAD18, commits cells to employs TLS, whereas TS induction requires PCNA poly-ubiquitination mediated by HLTF and SHPRH [43, 44].

THE DNA DAMAGE RESPONSE IN CANCER: FUNCTIONAL ASPECTS AND THERAPEUTIC CONSIDERATIONS

Mutations in DNA damage response genes and cancer predisposition

Given the fundamental role in maintaining genome preservation, it is not surprising that somatic or germline mutations in genes that participate to the DNA damage responses promote tumor formation. For example, about 15% of sporadic colorectal cancers (CRCs) show microsatellite instability (MSI) due to the inability of cells to repair DNA by using the MMR pathway [45] (see Chapter 3). This condition is also observed in a form of disease noted as hereditary non-polyposis colorectal cancer (HNPCC), a familial cancer predisposition (that is mainly conducive to the development of CRC), associated with loss-of-function mutations in mismatch repair genes such as *MSH2* and *MLH1* [46, 47].

In a different scenario, women with heterozygous germline mutations in *BRCA1* or *BRCA2* genes, involved in HR, are more prone to develop breast and ovarian cancers [48, 49]. Likewise, loss-of-function mutations in genes that regulate the response to DSBs are responsible of syndromic conditions that predispose to lymphomas. Examples are mutations in *ATM*, which causes ataxia telangiectasia; *MRE11*, which leads to ataxia telangiectasia-like disorder; and *NBS1,* associated with the Nijmegen breakage syndrome (NBS) [50]. Another example is xeroderma pigmentosum

(XP), a disorder that exhibits a > 1000-fold incidence of sun-induced skin cancer due to mutations in one of seven genes (*XPA–XPG*) involved in the NER pathway [51].

DNA damage response and therapeutic resistance

Beyond conferring susceptibility to cancer initiation, the DDR network is responsible for therapeutic resistance for many cancer types. Increasing evidence indicates that functional DDR pathways confer chemotherapy resistance by efficiently repair lesions produced by DNA-damaging agents. For example, DNA adducts generated by alkylating agents that generate a O^6-guanine methylations, such as temozolomide, dacarbazine and nitrosoureas, are quickly repaired by the MGMT alkyltranferase [52]. The higher levels of MGMT detected in tumor tissues suggest that its depletion, promoted by epigenetic silencing or the use of pseudo-substrates similar to O^6-methylguanine, may sensitize tumor cells to O^6-alkylating agents [53, 54]. Analogously, the BER repair pathway is therapeutically induced by IR, DNA-methylating agents, topoisomerase I poisons, such as camptothecin, irinotecan and topotecan, and some antimetabolites [55]. Thus, this pathway is an attractive target for the modulation of chemosensitivity, as shown by preclinical and clinical studies with different inhibitors. In this context, the most relevant compounds are AP endonuclease 1 (APE1) inhibitors and PARP inhibitors (discussed below) [56, 57]. Similarly, reactivation of silenced *MLH1* gene in the MMR pathway has been documented to promote chemosensitization [58]. DSBs generated by IR, radiomimetics and topoisomerase inhibitors are restored by DNA-PK-mediated NHEJ, a mechanism that contributes to chemo-radiotherapy resistance. So, selective DNA-PK inhibitors have been shown to sensitize cancer cell lines and xenografts to the antitumor activity of radiotherapy and chemotherapy [59-61].

Although the development of DDR inhibitors could enhance the cytotoxic effect of chemotherapy, such approach has some limitations as the overlapping DNA-repair pathways can

reduce agent activity and promote the acquisition of resistance mechanisms. Moreover, the combination of DDR inhibitors with conventional cytotoxic agents currently used in the clinic often shows elevated levels of toxicity. On this ground, the exploitation of DDR defects by synthetic lethality represents a promising land for a better development and application of DDR inhibitors for cancer therapy.

The principle of synthetic lethality: the paradigm of *BRCA*-deficient tumors and poly(ADP ribose) polymerase (PARP) inhibitors

Synthetic lethality describes the process by which defects in two gene products simultaneously lead to cell death, whereas individual inactivation of either of them does not affect viability. Observed firstly in *Drosophila* as recessive lethality [62], the mechanism has been exploited in cancer to unveil novel vulnerabilities on the basis of genetic defects [63]. To date, the relation between BRCA1/BRCA2 and PARP1 is the best know synthetic lethal relationship, in which the loss-of-function mutation of one gene (*BRCA1* or *BRCA2*) and the pharmacologic inhibition of the other (PARP1) prompt cancer cell death, whilst normal cells, lacking *BRCA1* and *BRCA2* gene mutations, are spared by the effect of the drug [64, 65].

The rationale behind the use of PARP inhibitors (PARPis) in the context of *BRCA*-deficient tumors stems from the function of PARP1 enzyme in sensing SSBs and mediating their repair [15]. Although initially thought to primarily inhibit global PARylation and thereby cause cytotoxicity, PARPis predominantly exert their antitumor activity by trapping PARP1. The consequence is the formation of DNA–protein crosslinks that trigger the collapse of replication forks upon encountering trapped PARP1, resulting in the accumulation of DSBs during the S phase of the cell cycle. *BRCA*-proficient cells employ HR to restore the DNA lesion. Conversely, *BRCA*-deficient cells are unable to repair the DNA break by HR, so they engage error-prone

pathways, such as c-NHEJ or aEJ, leading to the accumulations of chromosomal aberrations and cell death by mitotic catastrophe [64, 65].

To date, there are four small-molecule PARPis currently approved for clinical use: olaparib [66], rucaparib [67], niraparib [68] and talazoparib [69] for treatment of ovarian, breast, pancreatic [70] and prostate [71, 72] cancers. In addition, four PARPis are currently being tested in phase 3 trials (veliparib, pamiparib, fluzoparib and IMP4297), in monotherapy or in combination [73]. Approved PARPis differ in their ability to trap PARP1. Talazoparib is approximately 100 times more potent than niraparib, which traps PARP1 more potently than olaparib and rucaparib [74].

The clinical benefit of PARPis goes beyond tumors with germline or somatic mutations of *BRCA1* and *BRCA2* genes, as suggested by different trials showing that patients not harboring mutations in these genes have significant improvement by PARPi therapy. The administration of rucaparib in ovarian cancer patients with *BRCA1*/*BRCA2* wild type tumors that – however – display defects in other HR genes, increases median progression free survival (PFS) [75]. Similar results have been obtained in other phase 3 clinical trials using niraparib and olaparib [68, 76]. This evidence suggests that *BRCA1*/*BRCA2* mutations do not entirely account for the benefits derived from PARPi, and that deficiency in other HR genes confers sensitivity to this treatment. The notion that *BRCA1*/*BRCA2*-wild type tumors with poor activity of the HR pathway are susceptible to PARP blockade defines the concept of BRCAness, a phenotype demonstrated for ovarian [77, 78], prostate [79, 80] and other cancers [81]. Such condition is due to mutations in other genes beyond *BRCA1*/*BRCA2*, like *PALB2* [82, 83], *RAD51* homologues [84], *ATM*, *CHEK2*, *CDK12*, *FANCA*, *RAD54L* and *BRIP1* [81]. Moreover, mutations in key HR-unrelated DNA repair components or metabolic genes have been shown to increase sensitivity to PARPi. Examples are *ARID1A* [85], *BAP1* [86], *IDH1/2*, fumarase hydratase, and succinate dehydrogenases [87, 88].

In addition to combination with DNA-damaging chemotherapy and/or radiation, and their application in BRCAness tumors, PARPis have been tested in association with other DDR inhibitors, agents that target oncogenic proteins or with immune checkpoint therapies. For

example, olaparib-resistant cancer models can be resensitized to olaparib when combined with WEE1, ATR [89-91], or CHK1 inhibitors (NCT03057145). Similar benefit has been demonstrated by associating PARPis with androgen receptor inhibitors in castration-resistant prostate cancer [92-95]. Synergistic activity has also been observed in combination with PI3K/mTOR inhibitors [96-98], MEK inhibitors [99], anti-VEGF [100] and BET bromodomain (BRD4) inhibitors [101]. Finally, preclinical and clinical evidence suggests increased benefit when PARP inhibitors are associated to immunotherapy [102-106].

Beyond PARP: DNA damage repair proteins as targets for new therapeutic opportunities

The success of PARPis for synthetic lethality approaches has led to the exploration of other inhibitors that target different proteins involved in the DNA damage response. Differently from PARPis, most if not all the new drugs are currently in early clinical trials and, to date, not exploitable for routine clinical purposes. Among them, proteins that sense the DNA damage represent promising targets for the treatment of different tumor types. Four ATR inhibitors are currently in clinical trials: berzosertib (VE-822, VX-970 or M6620), ceralasertib (AZD6738), M4344 (VX-803) and BAY 1895344. Berzosertib has been the first ATR inhibitor to be evaluated in humans, and it has entered at least 19 registered phase 1 and 2 clinical trials that evaluate its efficacy in monotherapy or in combination with a large compendium of DNA-damaging agents and targeted therapies [107]. Similarly, ceralasertib, BAY 1895344 and M4344 are being tested as single agents or in combination with different chemotherapies in solid tumors (NCT03188965, NCT02278250). ATM, the other master sensor of DNA damage, represents another target for cancer therapy, as showed by the two currently inhibitors involved in clinical trials: AZD0156 and M3541. The latter is combined with radiotherapy in solid tumors (NCT03225105), whereas AZD0156 is tested in monotherapy and in combination with olaparib or 5-fluorouracil, folinic acid and irinotecan, in patients with advanced-stage solid cancers (NCT02588105). The DNA-PK inhibitors M9831 (VX-984), nedisertib (M3814, MSC2490484A) and CC-115 are presently

evaluated in phase 1 and 2 clinical trials as single agent or in combination with chemotherapy or radiotherapy in solid tumors (NCT02644278, NCT02316197, NCT02516813, NCT01353625, NCT02833883).

Beyond ATR, ATM and DNA-PK inhibitors, compounds targeting downstream targets have also been proposed. For instance, CHK1 and CHK2 inhibitors have long been studied for cancer treatment, but elevated toxicity has always been a limit, as shown by the double CHK1/CHK2 inhibitors UCN-01 [108, 109] and AZD6772 [110, 111] and by the CHK1 specific inhibitors rabusertib (LY2603618) [112], MK-8776 [113], prexasertib [114], GDC-575 (NCT01564251) and CCT245737 (NCT02797964, NCT02797977). Another important target is represented by WEE1, a protein kinase that regulate the G2/M checkpoint downstream from ATR and CHK1. Preclinical evidence showed that the WEE1 inhibitor adavosertib (AZD1775, MK-1775) sensitizes p53-deficient cells to chemotherapy and radiotherapy [115-117], which motivated the design of several clinical trials that are currently are ongoing [107]. Finally, DNA-pol θ inhibition has been demonstrated to be efficacious in both HR-deficient cells, through inhibition of the Alt-EJ pathway, and in cell lines with acquired PARP inhibitor resistance, through disruption of HR restoration [118].

Considering the reported studies, it is becoming increasingly clear that the rationale of synthetic lethality approaches can be applied also to different DDR inhibitors beyond PARP. For this reason, combinations between DDR inhibitors and/or other DNA-damaging agents are currently explored as upfront targeted treatments in chemorefractory patients and as advanced-line therapies to overcome therapy resistance in patients relapsed on PARPis.

COLORECTAL CANCER AND DNA DAMAGE RESPONSE: BIOLOGICAL, TRANSLATIONAL AND CLINICAL IMPLICATIONS

Genomic instability and multi-step progression

Colorectal cancer (CRC) is the third most frequent cause of cancer-related deaths in both the United States and Europe, accounting for approximately 10% of all annually diagnosed cancers and cancer-related deaths worldwide [119, 120]. Around 25% of individuals harbour metastatic disease (mCRC) at the time of diagnosis, while approximately 50% of patients will develop metastases later [121]. These epidemiologic data vary geographically, with the highest rates seen in the most developed countries, although a decreasing trend has been observed in recent years, mainly due to screening programs, lifestyle and dietary changes [122]. CRCs can be sporadic, with tumors occurring in individuals without a family history of CRC, or familial, due to inherited genetic mutations that increase CRC risk. The tumorigenesis process typically begins with an aberrant crypt, which evolves into a neoplastic precursor lesion (a polyp) and eventually progresses to colorectal cancer over an estimated range of 10–15year.

Sporadic colorectal cancer

Tumors can arise from two different evolutionary pathways characterized by different form of genomic instability (**Figure 4**). The first, accounting for 85-90% of sporadic tumors, presents a form of genomic instability called chromosomal instability (CIN), which causes an accelerated rate of chromosomal gains and losses with numerous changes in their copy number and structure [123]. The sequence of CIN events that leads to the evolution from normal epithelial cells to full-blown carcinoma is generally initiated by somatic inactivation of adenomatous polyposis coli (*APC*) gene, which triggers constitutive activation of the WNT-b-catenin oncogenic pathway, followed by activating mutations of the *KRAS* gene, *TP53* alterations, and loss of heterozygosity of the chromosome 18q locus (which contains genes encoding the SMAD effectors of TGFb

signaling). Phosphatidylinositol 3-kinase (PI3K, encoded by the *PI3KCA* gene) mutational activation is also frequent. CIN tumors are typically microsatellite stable (MSS) and display low levels of the CpG island methylation phenotype (CIMP), a form of epigenetic modification characterized by widespread promoter methylation [45].

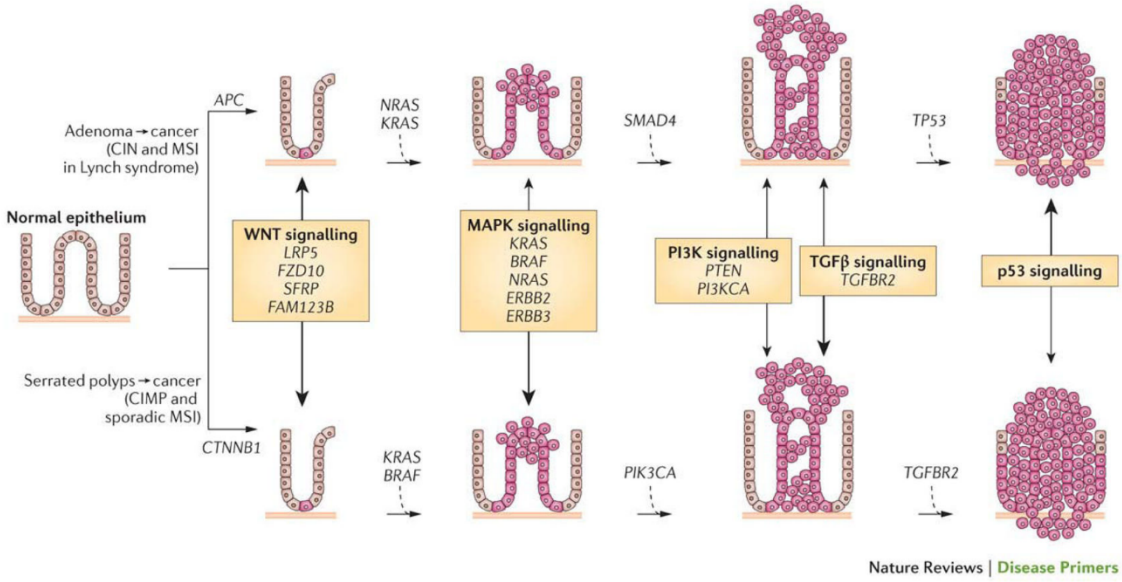

Figure 4. Evolutionary models of colorectal cancer. The main sequences of progression from normal colon to colorectal cancer show two forms of genomic instability, characterized by different genetic changes and histopathology. The 'classic' or traditional pathway (top) presents a form of genomic instability called chromosomal instability (CIN), which leads to the development of tubular adenomas that can progress to adenocarcinomas through the accumulation of genetic changes initiated by inactivation of the *APC* gene. Alteration of *KRAS*, *SMAD4* and *TP53* genes are events that classically contribute to the progression. The alternative pathway (bottom) is characterized by a genomic form of instability called microsatellite instability (MSI), due to genetic or epigenetic inactivation of MMR genes. Activating mutations of *BRAF* and CpG island methylation phenotype (CIMP) are characteristic of these tumors, although mutations affecting signaling components of the WNT–β-catenin pathway, PI3K, TGFβ and p53 often occur concomitantly with *BRAF* mutations. Adapted from Kuipers EJ et al., Nat Rev Dis Primers, 2015.

The remaining 10-15% of sporadic CRCs present a second, and less common, type of genomic instability named microsatellite instability (MSI) (**Figure 4**). When compared with MMS CRC, MSI tumors are characterized by different histopathological features (serrated polyps rather than tubular adenomas) and by distinct molecular events N [124]. These tumors predominantly arise in the right side of colon; are associated with *BRAF* mutations, a critical early event that leads to

uncontrolled cell proliferation through constitutive activation of the MAPK pathway; and in approximately 70% of cases exhibit a CIMP-high phenotype [45, 125] [126]. The sporadic MSI status is caused by an inefficient MMR machinery owing to genetic or epigenetic inactivation of MMR genes (in most cases, biallelic silencing of *MLH1* due to CpG island promoter hypermethylation). *BRAF* mutations are generally found in a mutually exclusive fashion with *KRAS* and *NRAS* mutations , while genes along the WNT–β-catenin, PI3K, TGFβ and p53 signaling pathways are commonly mutated or epigenetically silenced concomitantly with *BRAF* [127].

Hereditary colorectal cancer

About 5-7% of all CRC patients are affected by hereditary syndromes [128]. The commonest forms of hereditary CRC include familial adenomatous polyposis (FAP) and Lynch syndrome, also known as hereditary non-polyposis colorectal cancer (HNPCC). Both FAP and HNPCC are autosomal dominant disorders caused by monoallelic loss-of-function alterations of key oncosuppressor genes in the germline, followed by a somatic event that abrogates the functionality of the remaining wild type allele.

FAP is caused by inherited germline *APC* mutations (as opposed to acquired somatic *APC* mutations), with a histopathologic progression that follows the classic adenoma–carcinoma sequence and a genetic evolution superimposed to that of sporadic APC mutant CRC, including the frequent occurrence of *KRAS*, *TP53* and SMAD alterations and CIN [122]. HNPCC shows MMR deficiency – hence, an MSI phenotype – due to germline mutations in MMR genes, including *MLH1*, *MSH2*, *MSH6* and *PMS2* [129].

Treatment regimens in colorectal cancer

Surgery is the mainstay curative treatment for patients with non-metastatic CRC, and, in some cases, it is integrated by systemic treatments such as neoadjuvant and adjuvant approaches with radiotherapy, chemotherapy or chemoradiotherapy [130].

For metastatic CRC (mCRC), local treatment options, mainly for small and localized metastasis, are also considered and comprise surgery, radiofrequency ablation, microwave ablation or stereotactic radiotherapy [122]. However, the standard-of-care treatment for these patients includes cytotoxic agents and biological targeted compounds, which are administered cumulatively and – when possible – are tailored according to patient-specific and disease-specific predictive markers [131].

Targeted therapies

The EGFR monoclonal antibodies cetuximab and panitumumab are currently used in association with FOLXOX or FOLFIRI in the first- or second-line treatment of patients with *KRAS* or *NRAS* wild-type tumors [132]. The first-line treatment for mCRC patients harboring *KRAS* or *NRAS* mutations comprises either FOLFIRI or FOLFOX plus the anti-VEGF antibody bevacizumab [133, 134]. Beyond bevacizumab, two other anti-angiogenic drugs have been proved to positively impact on PFS and response rates when combined with chemotherapeutic agents in late lines of treatment: aflibercept (an anti-VEGF-A, VEGF-B, and placental growth factor) [135] and ramucirumab (an anti-VEGF receptor 2) [136]. Finally, heavily treated chemorefractory patients can experience slightly longer overall survival (OS) when treated with the multikinase inhibitor regorafenib, which also targets pro-angiogenic receptors [137].

Recently, a number of low-frequency aberrations in kinase-encoding genes have been identified in mCRC that result in constitutive activation of the corresponding protein products. Alterations in the *ERRB2* gene (mostly gene amplification) are detected in around 5% of *KRAS*, *NRAS* or

BRAF wild-type mCRCs and predict response to anti-HER2 combination therapies [138, 139]. Kinase fusions originating from chromosomal translocations and resulting in constitutive activation of neurotrophic receptor tyrosine kinase 1 (NTRK1), NTRK2, NTRK3, anaplastic lymphoma kinase (ALK), and RET account for approximately 1-2% of *KRAS*, *NRAS* or *BRAF* wild-type mCRCs. In this genetically defined tumor subset, inhibitors such as entrectinib (targeting NTRK, ROS1 and ALK) [140] and ponatinib (targeting various tyrosine kinases including RET) [141] have shown clinical activity. Tumors with *BRAF* gene alterations are found in 7-10% of mCRCs [127, 142] and are usually treated with the triplet chemotherapy FOLFOXIRI combined with bevacizumab [143]. Selective BRAF targeting with specific inhibitors has proven ineffective in patients with *BRAF* mutant mCRC due to feedback reactivation of EGFR signaling, which substitutes for BRAF blockade in stimulating the MAPK pathway [144, 145]. This observation has prompted the design of clinical trials aimed at evaluating the efficacy of combined BRAF and EGFR inhibition in patients with *BRAF* mutant mCRC. In a recent phase 3 study testing cetuximab and the BRAF inhibitor encorafenib versus cetuximab and irinotecan (or FOLFIRI), combined EGFR and BRAF blockade significantly improved response rates and OS compared with standard therapy. This superior activity was further enhanced by concomitant MEK inhibition [146].

Chemotherapy

The fluoropyrimidine antimetabolite 5-fluorouracil (5-FU) and leucovorin, a biomodulator that enhances 5-FU activity, are most often administered in combination with oxaliplatin, a platinum compound endowed with inter- and intra-strand DNA cross-linking activity (FOLFOX) [147], or irinotecan, a topoisomerase I inhibitor (FOLFIRI) [148]. The triplet combination FOLFOXIRI (5-FU/LV, oxaliplatin and irinotecan) is also considered [149]. Other therapeutic options include the fluoropyrimidine capecitabine plus oxaliplatin (CAPOX/XELOX) [150], capecitabine plus irinotecan (XELIRI) [151] and a modified XELIRI (mXELIRI) [152].

Potential determinants of response to chemotherapy have been brought to the fore based on the mechanism of action and metabolism of the various agents. However, the application of such predictors in clinical practice has been hampered by inconsistent results among different case series and poor diagnostic sensitivity and specificity. For some chemotherapeutics, in consonance with data from targeted therapies, drug target overexpression may be a positive determinant of sensitivity. For example, high expression of thymidylate synthase (TS), a direct target of 5-FU, has been associated with longer survival in CRC patients treated with adjuvant 5-FU-based therapy in some studies [153, 154]; however, other reports have not confirmed the positive predictive value of TS overexpression [155, 156] (**Table 1**). Likewise, elevated levels of topoisomerase I appear to predict better response to irinotecan [157] (**Table 1**). The activity of drug metabolic pathways is also thought to affect chemosensitivity. Dihydropyrimidine dehydrogenase (DPD) is a rate-limiting enzyme in fluoropyrimidine catabolism. High expression of DPD has been documented in tumors from patients with reduced sensitivity to capecitabine [158], with or without irinotecan [159], whereas inactivating polymorphisms of the *DYPD* gene (encoding DPD) have been associated with acute toxicity over the course of fluoropyrimidines-based therapy [160-162] (**Table 1**). In the same vein, deleterious polymorphisms of the *UGT1A1* gene (encoding glucuronosyltransferase, a key enzyme of irinotecan metabolism) are more frequent in patients who experience severe toxicity during treatment with irinotecan-based regimens [163, 164]

Responsiveness to chemotherapy may also be related to defects in DNA repair mechanisms after chemotherapy-induced DNA damage, leading to abnormalities in DNA replication and/or chromosome segregation that culminate in cancer cell death. Excision repair cross-complementation group 1 (ERCC1) is a key effector of DNA repair mechanisms and influences the tumor DNA-targeting effect of oxaliplatin. Some studies have shown that low transcript expression of the *ERCC1* gene correlates with longer survival of patients treated with FOLFOX [165] (**Table 1**). Similar findings were reported for an *ERCC1* polymorphism at codon 118, which

is expected to result in decreased *ERCC1* gene expression [166] (**Table 1**). These correlations, however, have not been confirmed in other datasets, especially when ERCC1 protein amounts rather than transcript expression was analyzed [167, 168].

Therapeutic agent	Biomarker	Analyzed in patients	Analyzed in preclinical models	Ref.
Chemotherapy				
Fluoropyrimidine (5-FU – Capecitabine)	▲ Thymidylate synthase (Resp)	YES	NO	153, 154
	▲ Dihydropyrimidine Dehydrogenase (Resist)	YES	NO	158, 159
Irinotecan	▲ Topoisomerase I (Resp)	YES	NO	157
	● *UGT1A1* (Tox)	YES	NO	163, 164
Oxaliplatin	▼ ERCC1 (Resp)	YES	NO	165, 166

▲ High expression ▼ Low expression ● Polymorphisms ★ Mutations

Resp, response; Resist, resistance; Tox, toxicity

Table 1. Validated and proposed biomarkers of response to chemotherapy regimen in mCRC. Adapted from Avolio and Trusolino, Cancer Discov., 2021.

DNA damage response pathways as response biomarkers and therapeutic targets in CRC

In some cases, genetic or functional defects in DNA damage response pathways are biomarkers of response to rational, molecularly driven anticancer therapies. In CRC, a paradigmatic example is represented by MSI tumors with MMR insufficiency. MSI tumors tend to accumulate nonsynonymous mutations; this increased mutational burden can translate into a higher neoantigen load, which makes some MSI tumors immunogenic and sensitive to immune checkpoint blockade [169]. Accordingly, single-agent therapy with the anti-PD-1 antibodies pembrolizumab or nivolumab and combination therapy with nivolumab and the anti-CTLA-4 antibody ipilimumab have been approved for treatment of patients with chemorefractory MSI mCRC [170-172].

Recent studies have documented germline and/or somatic genetic alterations in DDR genes other than MMR in CRC, ranging between 10% and 30% [173, 174]. As testified by the efficacy of blocking PARP/ssDNA repair in HR-deficient tumors harboring BRCA1/BRCA2 mutations or a BRCAness phenotype, defective DDR gene variants may pinpoint tumor subsets that are sensitive to synthetic lethality approaches with inhibitors of compensatory DDR pathways. Indeed, experiments in CRC cell lines have shown that *RAD54B* deficiency or *ATM* loss enhance responsiveness to olaparib treatment [175, 176] . Irrespective of underlying DDR gene mutations, a synergistic effect between PARPis and chemotherapeutics agents, such as oxaliplatin [177] and the active irinotecan metabolite SN-38 [178-180], as well as between ATM inhibitors and SN-38, has been demonstrated in CRC cell lines and patient-derived xenografts [181]. Likewise, concomitant blockade of CHK1 and MK2 (a downstream effector kinase of the ATM/ATR-dependent signaling network that operates in parallel to CHK1) leads to mitotic catastrophe and abrogates proliferation in *KRAS*- and *BRAF*-mutant cell lines [182].

The use of PARPi inhibitors in combination with genotoxic chemotherapeutics is being evaluated in clinical trials in mCRC patients, but remains problematic due to the elevated toxicity [183-185]. A large-scale drug screening conducted on 99 CRC cell lines resistant to anti-EGFR therapy showed that about 13% of the cell lines tested were sensitive to monotherapy with a PARPi, and response was strongly associated with oxaliplatin sensitivity [186]. Although single-agent activity of PARPis bodes well for clinical implementation of less toxic regimens, the identification of predictive biomarkers is needed to select for potential responders.

Interestingly, a recent study analyzed genomic and transcriptomic profiling of colorectal cancers to investigate the molecular and clinical characteristics of tumors exhibiting alterations in DDR pathways [187]. The authors showed a significant association between alterations in the DDR pathway and MSI status. In accordance with the observation that MSI tumors have a higher prevalence of *BRAF* mutations, *BRAF*-mutant tumors were significantly enriched for DDR

mutational profiles, whereas *KRAS*/*NRAS*-mutant tumors had a lower frequency of DDR mutations compared with *RAS*-wild type tumors.

In most cases, DDR gene alterations denote variants of unknown significance that may have deleterious consequences on the function of the encoded protein products on the basis of computational predictions. However, biological interrogation of the identified mutations is necessary to validate the predicted loss of function phenotype. A better understanding of the DDR machinery, combined with improved functional testing and sequencing technologies, could lead to the exploitation of DDR deficiency for combination therapies with other DNA-damaging agents in molecularly defined mCRC patient subsets.

AIM OF THE WORK

The refinement of surgical techniques and the use of more effective systemic therapies have increased the life expectancy of patients with metastatic colorectal cancer (mCRC). However, advanced-stage colorectal tumors are still a leading cause of cancer related-deaths. Although the implementation of genomic analysis and the ensuing identification of molecular determinants of response have helped to enrich for potential responders to targeted therapies, approaches of this kind have been unsuccessful for chemotherapy, in part due to its often incompletely understood and diverse mechanisms of action. Lack of predictive biomarkers for improved stratification of molecularly defined patient subgroups to chemotherapeutic regimens calls for a better knowledge of the activity of chemotherapeutic agents and highlights the need to identify clinical-grade determinants of response.

Responsiveness to chemotherapy may be related to defects in DNA repair mechanisms after chemotherapy-induced DNA damage, leading to abnormalities in DNA replication and/or chromosome segregation that culminate in cancer cell death. On this ground, the aim of this work is to dissect the role of DNA damage response (DDR) signaling as a modulator of sensitivity and resistance to chemotherapy in mCRC, using patient-derived models (xenografts and organoids) as experimental tools. This information is also expected to deliver predictive biomarkers with clinical applicability as a means to better inform clinical decision making.

The objective of rationalizing the use of chemotherapy on a molecular basis goes along with the appreciation that many DDR molecules may be therapeutic targets. Indeed, starting from the notion that *BRCA*-mutant cancer cells are sensitive to inhibition of poly (ADP-ribose) polymerase, the landscape of antitumor agents targeting the DDR protein domain is constantly

growing. Accordingly, a parallel aim of this study is to nominate DDR-related signals as stand-alone or synergistic vulnerabilities, which may either substitute for or enhance the effect of chemotherapeutic drugs.

Ultimately, a clearer understanding of the cellular and molecular underpinnings of chemotherapy activity in clinically relevant experimental models will be key to credentialing functional response biomarkers above and beyond descriptive variables in patients.

RESULTS

Patient-derived xenografts treated with FOLFIRI recapitulate response rates observed in the clinic

To unveil potential determinants of response to chemotherapy, we firstly explored if patient-derived xenografts (PDXs) could be a reliable methodological resource for this effort. Consequently, we generated a large platform of molecularly-annotated mCRC PDXs, using a set models collected in the past years and already exploited in independent studies [188, 189] to assess the sensitivity to FOLFIRI treatment.

The trial was performed on 75 mCRC samples that had successfully engrafted after thawing from the archive. Xenografts were propagated until production of treatment cohorts of 5 mice from each implanted specimen. When tumors in each cohort reached an average volume of 400 mm^3, mice were randomized to receive either placebo or FOLFIRI. For assessment of tumor response to therapy, we used volume measurements and adopted a classification methodology loosely inspired by clinical criteria: (i) tumor regression (or shrinkage) was defined as a decrease of at least 50% in the volume of target lesions, taking as reference the baseline tumor volume; (ii) at least a 35% increase in tumor volume identified disease progression; and (iii) responses that were neither sufficient reduction to qualify for shrinkage nor sufficient increase to qualify for progression were considered as disease stabilization.

Endpoint was scheduled 6 weeks after treatment initiation. At this evaluation timepoint, 24 cases (32%) had tumor shrinkage, 27 cases (36%) disease stabilization, and 24 cases (32%) tumor progression (**Figure 5**). When analyzing the prevalence of the most frequent and/or prognostically relevant CRC oncogenic mutations (*KRAS*, *NRAS*, *BRAF*) in the different response categories, a trend towards an enrichment for *KRAS* mutations in resistant cases could be appreciated (9/24 in resistant models, 37.5%; 4/24 in sensitive models, 16.7%) (**Figure 5**). The response distributions

observed in this trial were in agreement with those observed in patients treated with FOLFIRI [190], attesting to the value of the platform as a preclinical tool for biomarker discovery and patient stratification in the context of chemotherapy. Of note, the patients included in our collection underwent potentially curative metastasectomy, so in most cases they were not treated with FOLFIRI and we do not have matched information on therapeutic response between PDXs and donor patients.

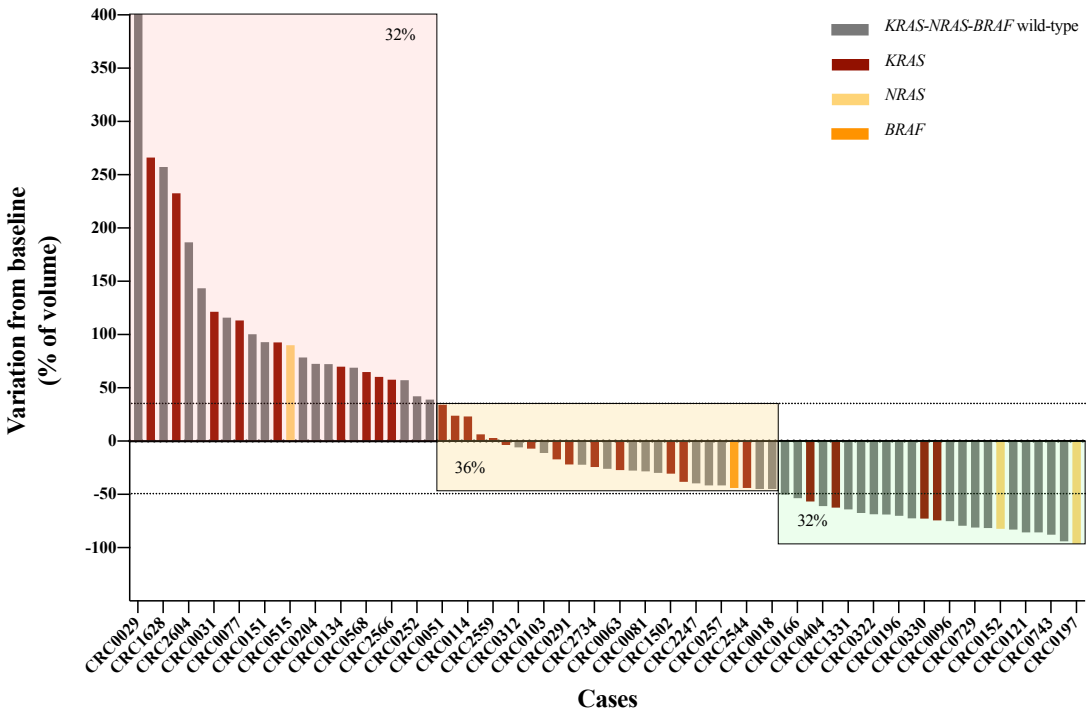

Figure 5. **FOLFIRI response rates in mCRC PDXs are analogous to those observed in patients.** Waterfall plot of response after 6 weeks of treatment with FOLFIRI (25 mg/Kg twice a week intraperitoneally in combination with 5-FU 100 mg/Kg once a week intraperitoneally), compared with tumor volume at baseline, in a population of 75 PDX models (n = 5 mice for each bar). Dotted lines indicate the cutoff values for arbitrarily defined categories of therapy response: regression (below the lower line, −50%), progressive disease (above the upper line, +35%), and stabilization (between the lines). Bars are colored according to the mutational status of *KRAS*, *NRAS* and *BRAF* genes.

FOLFIRI-induced DNA double strand-breaks are higher in sensitive tumors

The topoisomerase I (TOP1) inhibitor irinotecan, a soluble derivate of camptothecin, is a key component of FOLFIRI.

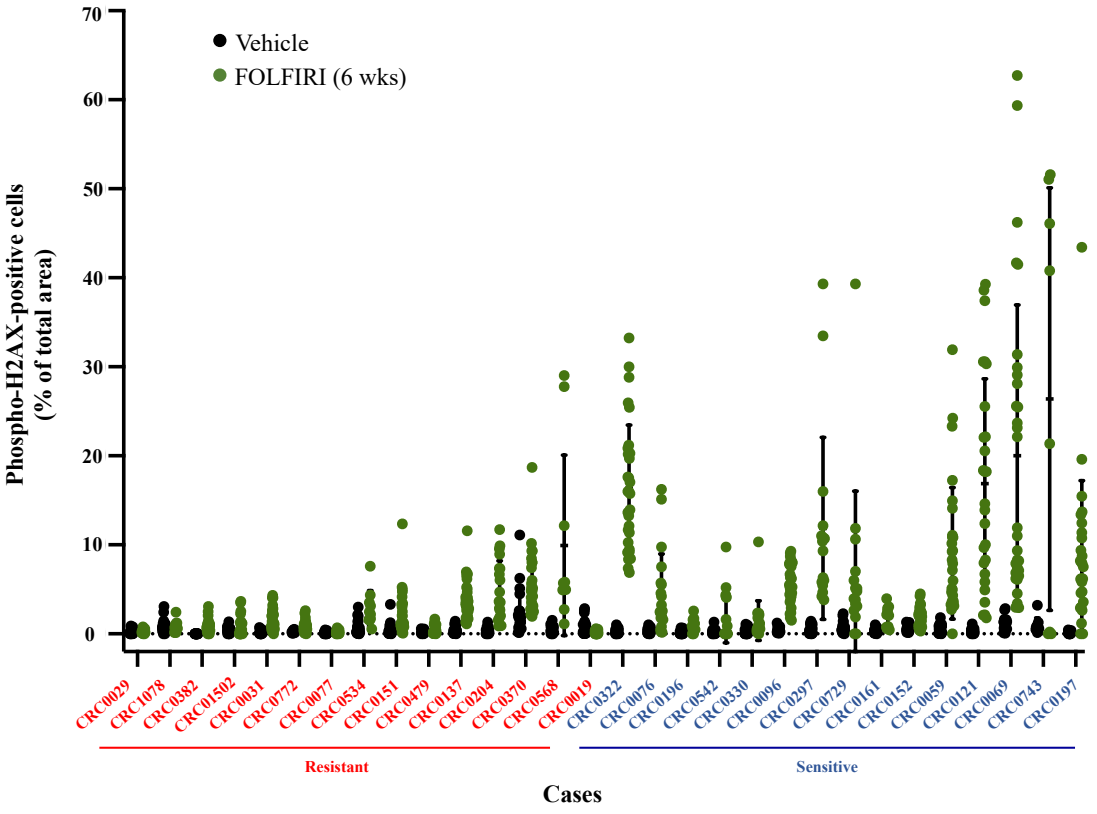

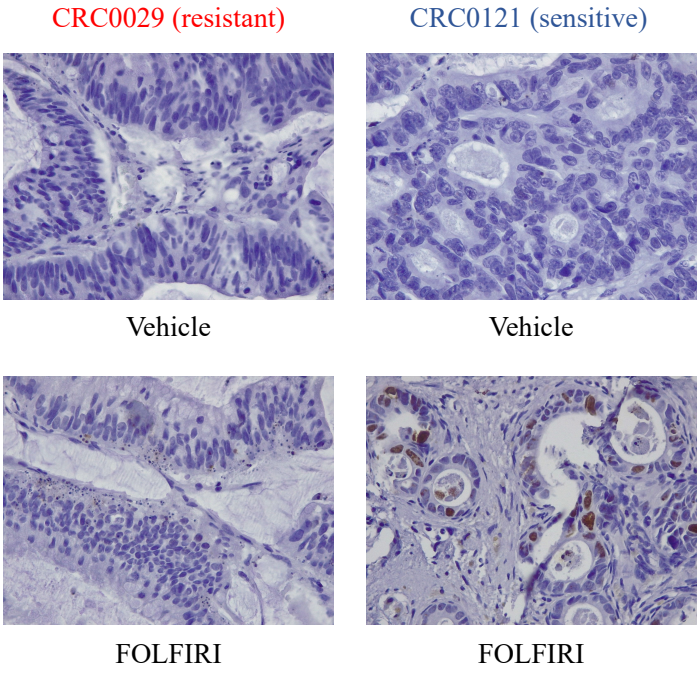

Figure 6. Double-strand DNA break formation in PDXs correlates with FOLFIRI response. Top, morphometric quantification of nuclear γ-H2AX positive tumor cells in basal condition (black dots) and upon 6 weeks of treatment with FOLFIRI (green dots). Each dot represents the average of 10 optical fields (40X) randomly chosen from each tumor. **Bottom**, representative images of γ-H2AX immune-staining of one resistant and one sensitive tumor model treated with vehicle or FOLFIRI for 6 weeks. Original magnification: 400X

Physiologically, TOP1 removes DNA negative supercoiling, a step necessary for DNA replication, by nicking the DNA, enabling the broken strand to rotate around the TOP1-bound DNA strand. The cleavage intermediate is referred to as a cleavage complex (TOP1cc) because TOP1 cleaves DNA by forming a covalent bond to the 3′ DNA terminus. Irinotecan selectively binds the TOP1cc during DNA replication, and when DNA polymerases encounter the trapped TOP1cc, a DNA double-strand break is generated [191].

One of the first factors activated by DSBs is the histone variant H2AX, which once phosphorylated at the serine 139 residue (γ-H2AX) promotes the accumulation of other DNA repair proteins around the DSB site [19]. Thus, to examine DSB production after irinotecan treatment, and whether the extent of DSB abundance correlates with therapeutic response, we performed an immunohistochemical analysis of end-of-treatment PDX FFPE samples to detect γ-H2AX positivity as a pharmacodynamic proxy for DNA DSB formation [192, 193]. For this analysis, we chose the extreme tails of response distribution, specifically the 15 most sensitive and the 15 more resistant models. Our results showed that the levels of γ-H2AX were higher in sensitive than in resistant tumors after prolonged treatment with FOLFIRI (**Figure 6**). Notably, a general trend was apparent whereby the "less resistant" tumors among chemorefractory tumors, as well as the most sensitive tumors among responders, were those displaying the most marked increase in γ-H2AX positivity within their category after irinotecan administration (**Figure 6**; models are ranked for increasing sensitivity, for each response category, from left to right). The reduced formation and persistence of DSBs in FOFLIRI-resistant tumors suggests that poor response to irinotecan may be due to more pronounced DSB repair proficiency, which protects cancer cells from the catastrophic consequences of massive DNA damage, hence from cell death.

Irinotecan-sensitive PDX-derived organoids accumulate more DSBs upon treatment

To further validate this observation in a methodological context more prone to experimental manipulation, we carried out a parallel analysis by exploiting our platform of PDX-matched organoids.

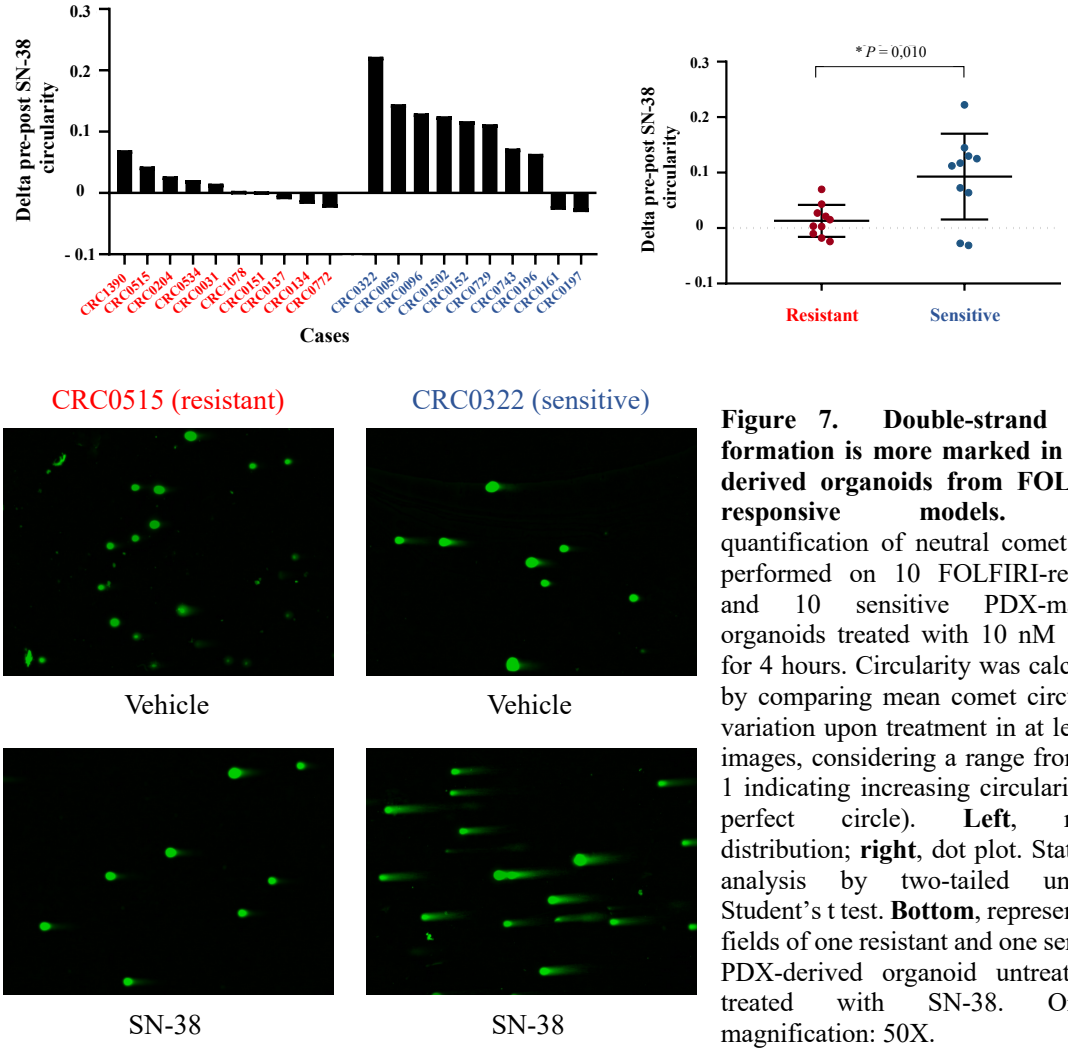

Figure 7. Double-strand break formation is more marked in PDX-derived organoids from FOLFIRI-responsive models. Top, quantification of neutral comet assay performed on 10 FOLFIRI-resistant and 10 sensitive PDX-matched organoids treated with 10 nM SN-38 for 4 hours. Circularity was calculated by comparing mean comet circularity variation upon treatment in at least 50 images, considering a range from 0 to 1 indicating increasing circularity (1= perfect circle). **Left**, ranked distribution; **right**, dot plot. Statistical analysis by two-tailed unpaired Student's t test. **Bottom**, representative fields of one resistant and one sensitive PDX-derived organoid untreated or treated with SN-38. Original magnification: 50X.

In this case, we assessed the extent of irinotecan-induced DSBs in our organoid models using a single cell gel electrophoresis assay, known as comet assay [194]. This is a simple method for measuring DNA strand breaks in eukaryotic cells. Cells embedded in agarose on a microscope slide are lysed with detergent and high salt to form nucleoids containing supercoiled loops of DNA linked to the nuclear matrix. Electrophoresis at high pH results in structures resembling

comets, observed by fluorescence microscopy; the intensity of the comet tail relative to the head reflects the number of DNA breaks. The likely basis for this is that loops containing a break lose their supercoiling and become free to extend toward the anode.

Data from the comet assay in organoids proved to be consistent with results in PDXs; indeed, similar to the in vivo setting, organoids derived from FOLFIRI-resistant PDXs were less prone to accumulate DSBs caused by the active metabolite of irinotecan SN-38. Conversely, organoids obtained from FOLFIRI-sensitive PDXs showed high levels of DSBs (**Figure 7**). This corroborates the notion that sensitivity to irinotecan associates with more prominent DSB formation after the genotoxic insult.

Organoids from FOLFIRI-sensitive tumors show functional signs of BRCAness

Results obtained in PDXs and organoids show a clear segregation between cases with high levels of DSBs and cases with low levels of DNA damage upon FOLFIRI treatment, which respectively associate with response and resistance to therapy. Since DSBs are typically repaired by the homologous recombination pathway, we hypothesized that defects in HR may underlie the inability of tumors displaying exquisite sensitivity to the drug to repair irinotecan-induced DSBs.

As mentioned in the Introduction, HR-deficient tumors exhibiting loss-of-function mutations of BRCA1/2 or a BRCAness phenotype (genetic or non-genetic hallmarks of functional inactivation of HR genes) show exquisite sensitivity to PARP1 blockade. This synthetic lethal interaction is caused by the inability of HR-deficient cells to repair the DSBs produced by the collapse of replication forks, which in turn is triggered by PARP inhibition. On this ground, we reasoned that an approach to test HR proficiency/deficiency in our models could be by assessing their susceptibility to PARP1 pharmacologic inactivation. Our results showed that, overall, organoids derived form FOLFIRI-resistant tumors were less sensitive to the PARP inhibitors olaparib and niraparib (**Figure 8A, 8B**).

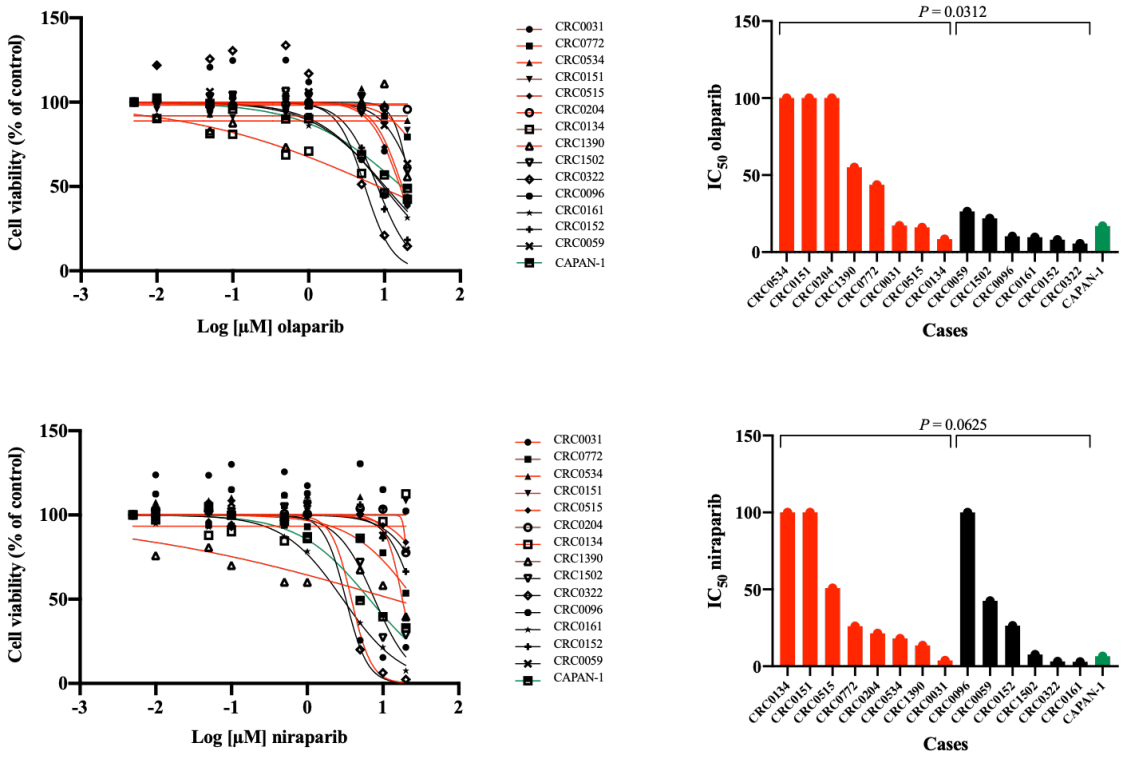

Figure 8. The effect of PARP blockade in PDX-derived organoids correlates with FOLFIRI response. Left, pharmacologic response to olaparib (**top**) and niraparib (**bottom**) in 14 PDX-derived organoids treated for 7 days at the indicated concentrations (μM). CAPAN-1, a BRCA2-deficient pancreatic cell line, was used as positive control. Red and black curves represent organoids derived from PDXs that showed resistance or sensitivity to FOLFIRI treatment *in vivo*, respectively. Green denotes the positive control. Organoid viability was measured by CellTiter GLO assay. **Right**, IC_{50} of organoids in response to olaparib (**top**) and niraparib (**bottom**) calculated by non-linear regression using Graphpad Prism software. Bars are colored considering the response of PDXs to FOLFIRI *in vivo* (red, resistance; black, sensitivity), and organoids are ranked based on the higher value of IC_{50}. Green bar represents IC_{50} of CAPAN-1 cell line. Results are the average of at least two independent experiments, each performed in technical triplicate. Statistical analysis by two-tailed Wilcoxon test.

Conversely, organoids derived form FOLFIRI-sensitive tumors showed increased sensitivity to either PARP inhibitor. These data reinforce our working hypothesis whereby proficiency of the HR pathway – here documented by reduced response to PARP inactivation – plays a pivotal role in mediating chemoresistance in mCRC.

RAD51 is basally more expressed in resistant tumors and becomes more active after FOLFIRI treatment

RAD51 is a key recombinase of the HR pathway. Importantly, RAD51 expression has predictive capacity to discriminate PARPi-sensitive *versus* PARPi-resistant mammary tumors [195, 196]. This piece of information has fostered the idea of including RAD51 protein expression analysis in the toolbox of surgical pathologists as a functional biomarker of homologous recombination proficiency for patient stratification to PARPi therapy.

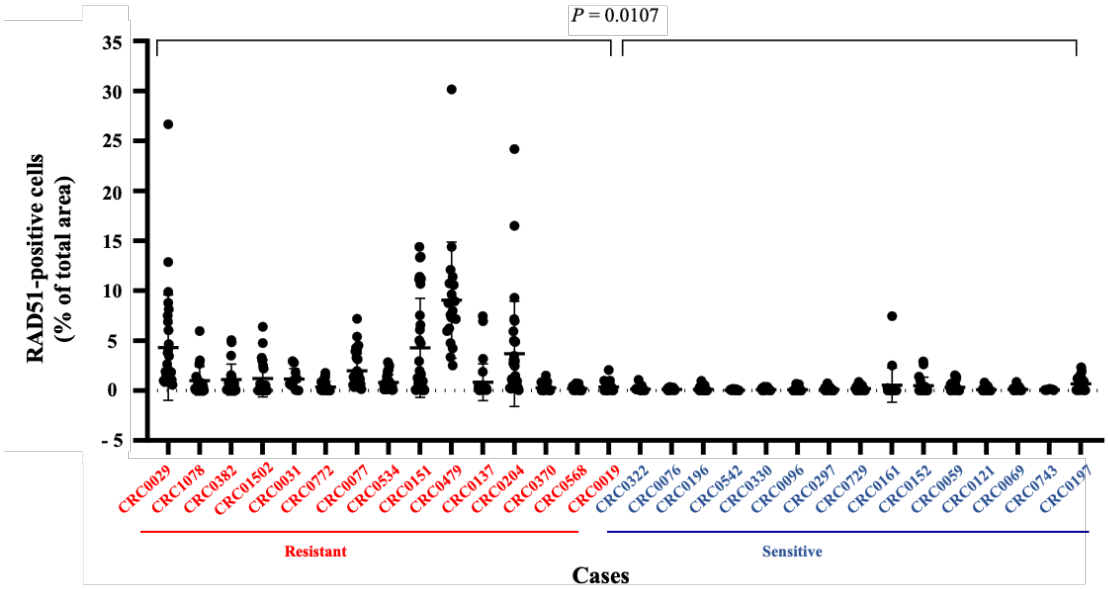

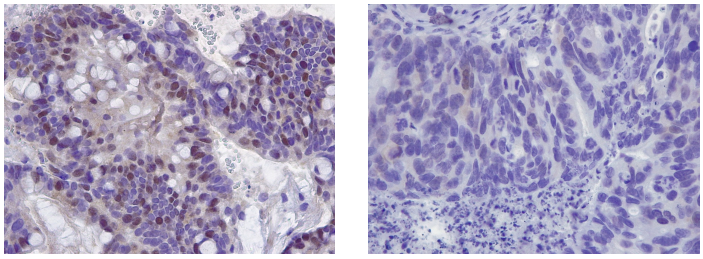

Figure 9. RAD51 is more expressed in FOLFIRI-resistant tumors. Top, morphometric quantification of basal RAD51 expression in the same cohort of PDXs analyzed for γ-H2AX positivity. Each dot represents the average of 10 optical fields (40X) randomly chosen from each tumor. Statistical analysis by two-tailed unpaired Welch's *t* test. **Bottom**, representative images of RAD51 immunostaining of one resistant and one sensitive tumor model in untreated condition. Original magnification: 400X.

On these premises, and based on our results showing less DSB formation and less response to PARP blockade in chemoresistant mCRC, we investigated RAD51 expression in our collection

of therapeutically annotated PDXs, specifically, in the same 15 FOLFIRI-resistant and 15 FOLFIRI-sensitive models already tested for γ-H2AX detection.

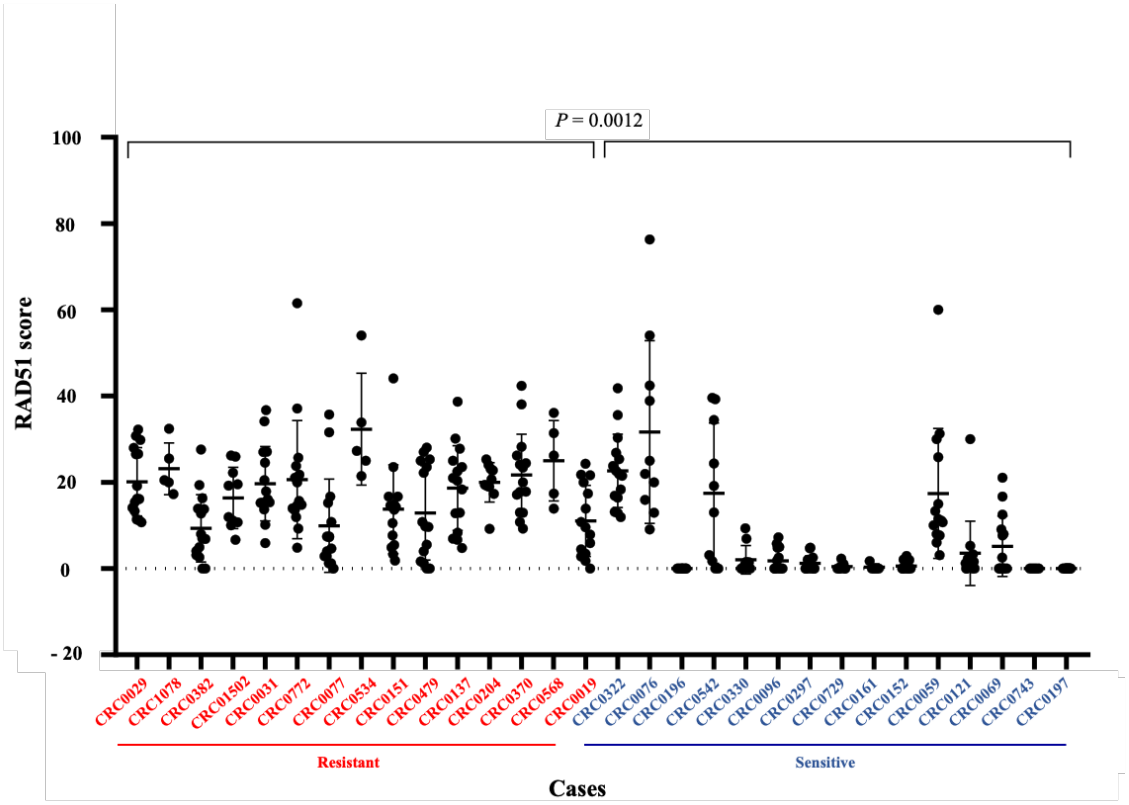

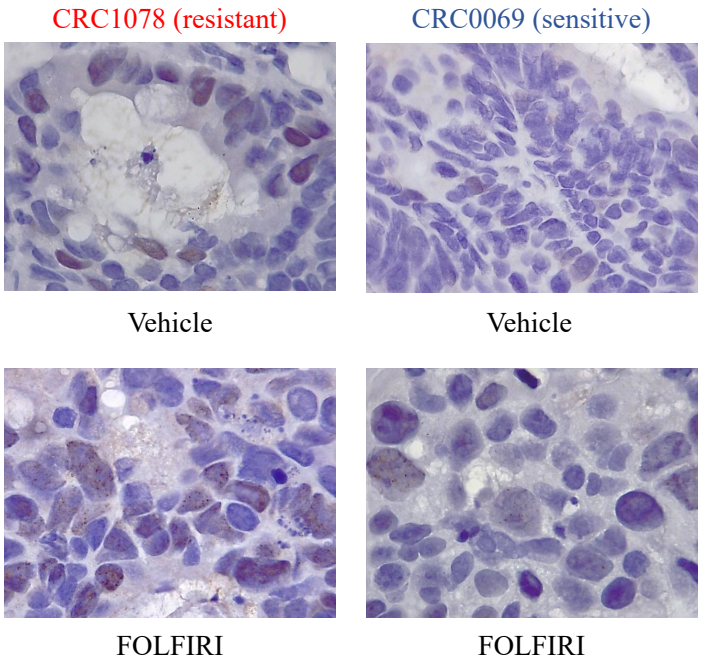

Figure 10. RAD51 is more activatable in FOLFIRI-resistant tumors. Top, analysis of RAD51 score of tumors after FOLFIRI treatment for 6 weeks. RAD51 was quantified by scoring cells with ≥2 foci/cell. Each dot represents the average of 10 optical fields (40X) randomly chosen from each tumor. Statistical analysis by two-tailed unpaired Welch's t test. **Bottom**, representative images of RAD51 immunostaining of one resistant and one sensitive tumor model in untreated conditions and after FOLFIRI treatment. Original magnification: 400X.

Immunohistochemistry results showed that the basal levels of RAD51 in resistant PDXs were higher than in sensitive models (**Figure 9**). Furthermore, treatment with FOLFIRI induced the congregation of RAD51 in nuclear foci – indicative of HR pathway activation – in all the resistant, but not in most of the sensitive, PDXs (**Figure 10**).

These findings suggest that chemoresistance relies on the ability of some mCRC tumors to empower faster and more efficient repair of the DSBs by engaging the HR pathway after genotoxic stress. Resistant and sensitive tumors showed heterogeneous basal mRNA levels of RAD51 irrespective of FOLFIRI response, ruling out a transcriptional regulation of the differential protein expression of the recombinase in resistant *versus* sensitive tumors (**Figure 11**).

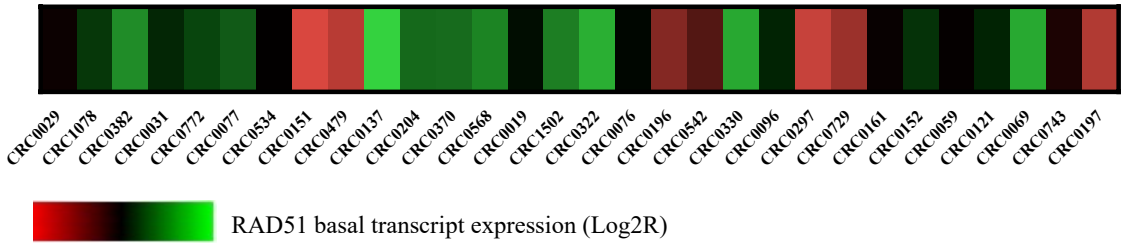

Figure 11. Differences in RAD51 protein expression do not correlate with RAD51 transcript levels in PDXs. RAD51 mRNA expression measured by RT-qPCR in resistant and sensitive tumor xenografts in basal conditions. Cases are ranked from the most resistant (CRC0029) to the most sensitive (CRC0197) to FOLFIRI treatment *in vivo*.

Basal cell cycle dynamics are different in chemosensitive and chemorefractory tumors, and are differentially affected by therapy

Irinotecan exerts its genotoxic effect during the S phase of the cell cycle. Likewise, HR-mediated DNA damage response occurs in the post-DNA replication segment of the cell cycle, during the late S and G2 phases. To explore whether the steady-state and therapy-induced kinetics of cell cycle progression were different in chemoresistant *versus* chemosensitive tumors, we evaluated

the basal and post-treatment distribution of the various phases of the cell cycle using the expression pattern of phase-specific cyclins as a pharmacodynamic readout.

Our immunohistochemical data showed that, under basal conditions, sensitive tumors with low RAD51 activity displayed a higher number of cells engaged in the phases of active DNA replication and mitosis than resistant, RAD51-overexpressing tumors (**Figure 12A**). This indicates that sensitive tumors cycled faster that resistant tumors, consistent with that documented in clinical experience. After FOLFIRI, sensitive tumors showed a marked reduction of cells in S, G2 and M phases compared with resistant models (**Figure 12B**).

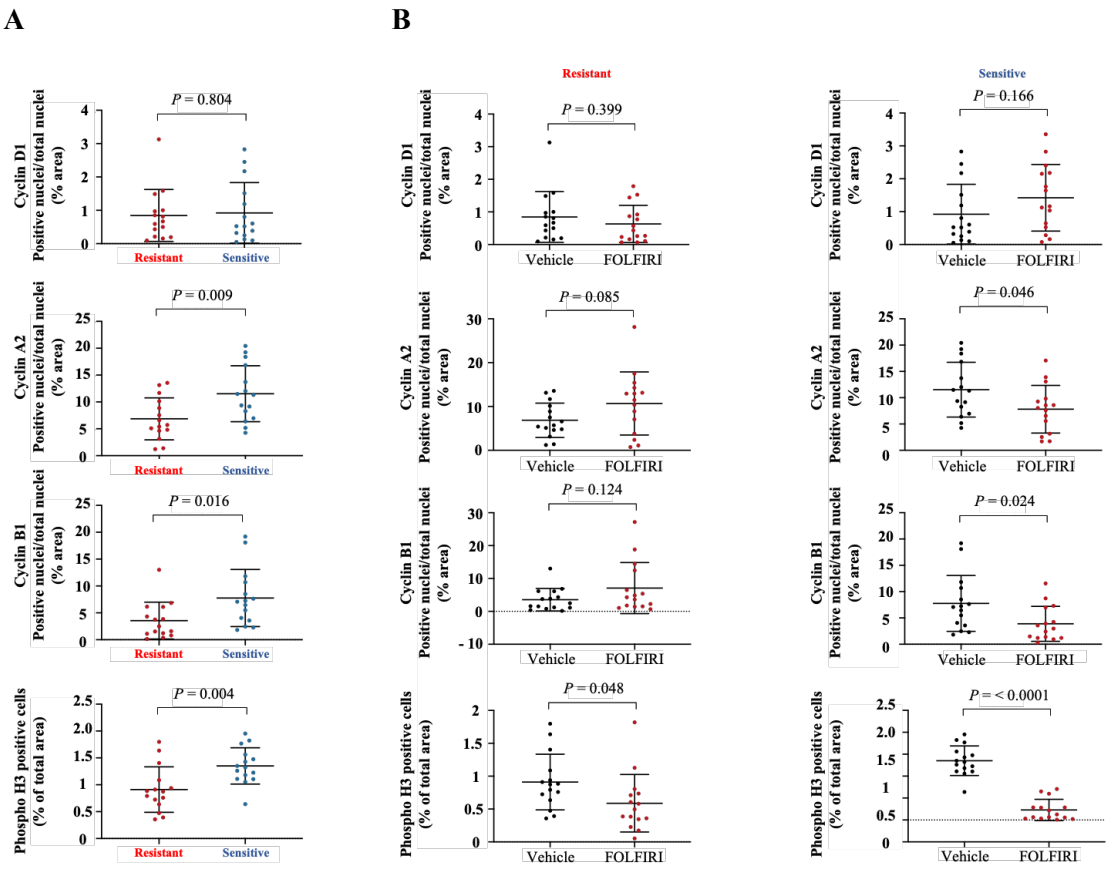

Figure 12. Dynamics of cell-cycle progression in PDXs are different in FOLFIRI-resistant and sensitive PDXs. (A) Quantification of cell-cycle distribution in resistant (red dots) and sensitive (blue dots) tumors in basal conditions, based on immunohistochemistry analysis of cell-phase-specific cyclin expression. **(B)** Quantification of cell-cycle distribution in vehicle-treated (black dots) and FOLFIRI-treated (red dots) PDXs, after 6 weeks of therapy, in resistant and sensitive tumors. Each dot represents the average of 10 optical fields (40X) randomly chosen from each tumor. Phase G1= cyclin D1, phase S= cyclin A2, phase G2= cyclin B1, mitosis= phospho-H3 Statistical analysis by two-tailed unpaired Student's t test.

A plausible interpretation for these findings is that steady-state rapidly cycling mCRC tumors are susceptible to the genotoxic effect of irinotecan by actively and repeatedly entering the S-phase "danger zone", in which irinotecan-triggered DNA damage cannot be contrasted because RAD51 levels are low and HR activity is suboptimal. This leads to abortive cell cycle progression, with only few cells experiencing the subsequent post-replication phases and a strong reduction in the positivity for S-phase and M-phase markers. In slowly-cycling tumors with high RAD51 expression, the DNA-damaging activity of irinotecan is probabilistically reduced by the fact that a lower number of cells enter S phase, and by the possibility for cells in S phase to empower RAD51-dependent DNA repair and progress through the cell cycle.

ATR mutations are potential vulnerabilities in metastatic CRC

To gain further insight into the interplay between HR deficiency and chemosensitivity, we subjected 44 PDX models to targeted NGS for a manually curated panel of 33 genes implicated in the HR pathway. Except for 5 genes, all other members of the HR pathway proved to be mutated at variable frequencies (**Figure 12A**).

Mutations were mainly heterozygous and included both missense and nonsense variants, and require functional characterization for better understanding their potential impact on chemosensitivity.

In general, there was no evident segregation in the mutational prevalence between sensitive and resistant models. However, the ataxia telangiectasia and Rad3-related (*ATR*) gene stood out for the specific enrichment of mutations among refractory cases (**Figure 13**). The association between ATR mutations and chemoresistance was substantiated at the population level by extending the mutational analysis to a wider set of PDXs (Figure 13).

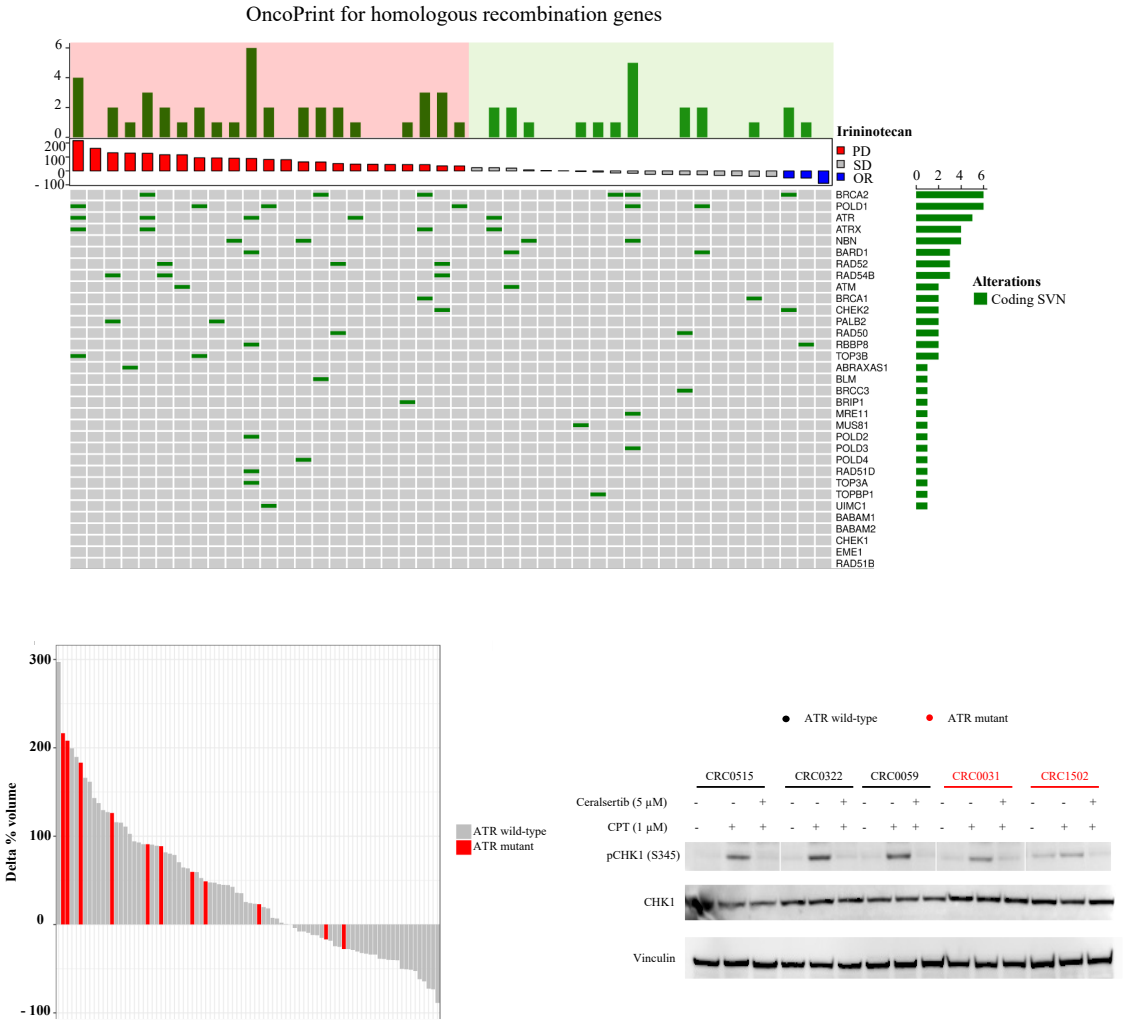

Figure 13. Mutational landscape of HR genes identifies ATR mutations in chemorefracrory tumors. **Top**, OncoPrint depicting HR genomic alterations (33 genes) in 44 PDX models. Tumors were stratified based on FOLFIRI response (PD, progressive disease; SD, stable disease; OR, objective response). **Bottom left**, mutational analysis of n = 86 PDXs showing *ATR*-mutated cases (red bars), stratified onto response annotation (waterfall plot). **Bottom right**, Western blot analysis of p-CHK1 Ser 473 and CHK1 total protein expression in *ATR* wild-type (black) and *ATR*-mutant (red) organoids. Cells were treated with the indicated concentrations of camptothecin (CPT), ceralasertib, or the combination of both for 4 hours. Vinculin was used as a loading control.

As mentioned in the Introduction, ATR is a sensor of DSBs (like ATM) but also responds to many other types of genotoxic stress. ATR is essential for the viability of human cells [27]; consistently, the *ATR* mutations detected in our models were heterozygous, suggesting a potential hypomorphic phenotype compatible with life. Accordingly, we found that camptothecin-dependent activation

of ATR – as assessed by phosphorylation of the ATR downstream substrate CHK1 – was weaker in *ATR*-mutant than in *ATR* wild-type organoids (**Figure 13**).

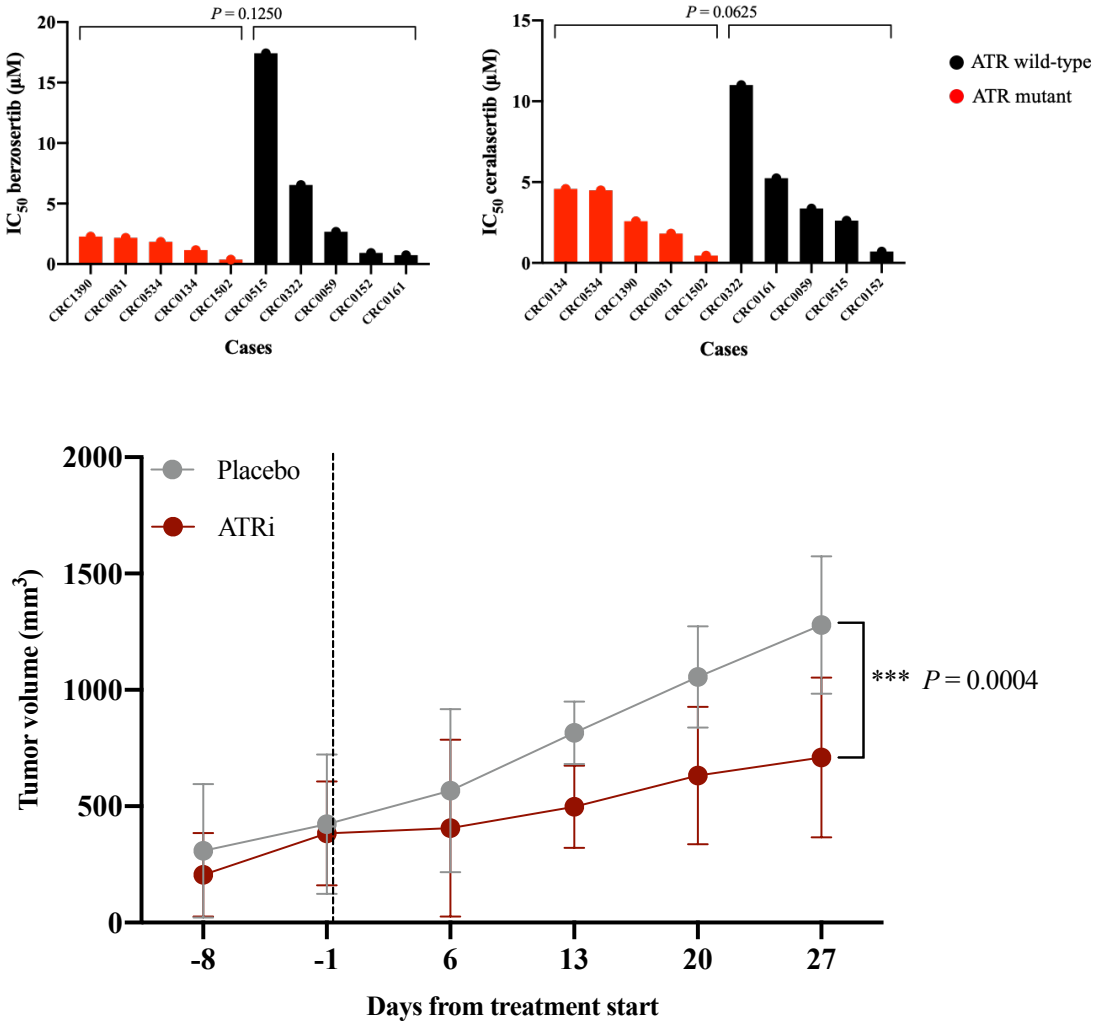

Figure 14. ATR is a druggable target in ATR mutant chemorefracrory tumors. Top, IC_{50} of organoids in response to berzosertib (left) and ceralasertib (right) calculated by non-linear regression using Graphpad Prism software. Cells were treated with increased concentrations (from 0 to 20 μM) of ATR inhibitor for 7 days and viability was measured by CellTiter GLO assay. Bars are colored considering the *ATR* mutational status (black, wild-type; red, mutated) and organoids are ranked based on the higher value of IC_{50}. Results are the average of at least three independent experiments, each performed in technical triplicate. **Bottom**, Tumor growth curves of CRC1502 ATR mutated mCRC xenograft treated with placebo (gray curve) or the ATR inhibitor ceralasertib (red curve) (50 mg/kg daily by oral gavage). $n = 4$ to 6 animals for each treatment arm. Error bars indicate SEM. Statistical analysis by two-way ANOVA.

We reasoned that ATR partial loss of function may render *ATR*-mutant tumors particularly susceptible to full ATR inactivation by ATR chemical inhibitors. This assumption is supported by the notion that the ATR-CHK1 pathway counteracts RAD51 ubiquitylation and degradation

[197]. Therefore, ATR inhibition would suppress not only the DNA repair function of ATR through direct chemical hindrance, but also that of RAD51 through protein downmodulation, an effect that could be particularly detrimental in RAD51-overexpressing chemoresistant tumors.

We investigated the role of mutant ATR as a potential target in chemorefractory mCRC by conducting pharmacological inhibition of ATR in PDX-matched organoids. Our results showed that *ATR*-mutant organoids were more sensitive to the activity of berzosertib and ceralasertib, two ATR inhibitors currently under clinical experimentation, than ATR wild-type organoids (**Figure 14**). Of note, sensitivity to ATR blocked was confirmed in vivo: although monotherapy with ceralasertib did not induce overt tumor regression, the treatment potently delayed tumor growth (**Figure 14**). Collectively, these results highlight the value of *ATR* mutations as predictors of resistance to FOLFIRI and predictors of response to ATR-targeting agents. Future work is needed to explore whether ATR blockade is sufficient to instate sensitivity to FOLFIRI in *ATR*-mutant chemorefractory tumors.

DISCUSSION

Colorectal cancer is still a leading cause of cancer related-deaths worldwide; in particular, patients with metastatic disease represent a major obstacle to treatment benefit. Indeed, although advances in the diagnosis and treatment of unresectable metastatic CRC have enabled the personalization of patients‘ care, less than 20% of mCRC patients survive beyond 5 years [119]. Chemotherapy remains the standard-of-care treatment for these patients. However, the incomplete knowledge of chemotherapy action and the substantial lack of predictive biomarkers of response greatly contribute the dismal outcome of subjects with metastatic colorectal cancer. As mentioned in the Introduction, potential determinants of response to chemotherapy have been proposed based on the mechanism of action and metabolism of the various agents. However, the application of such predictors in clinical practice has been hampered by inconsistent results among different case series and poor diagnostic sensitivity and specificity [131]. For this reason, a clearer understanding of the cellular and molecular underpinnings of chemotherapy activity in clinically relevant experimental models is a necessary prelude to the nomination of response biomarkers above and beyond descriptive variables in patients. On this ground, we took advantage of patient-derived platforms, namely PDXs and PDX-matched organoids, to investigate the mechanisms underlying chemotherapy resistance in mCRC. Because the chemotherapeutic regimens used in CRC are genotoxic drugs rather than antimitotic agents, we focused on exploring the contribution of the DNA damage response pathway to dictating chemotherapy sensitivity.

Firstly, we provided evidence that our PDX platform is a reliable preclinical tool for understanding therapeutic response in mCRC. By conducting large-scale xenotrials, we observed that the response of the tumor population to FOLFIRI treatment showed a polarized distribution, with response rates analogous to those observed in patients [190]. These data corroborate previous observation obtained in our laboratory on the same cohort of tumors, in which a systematic survey

of *KRAS* and *NRAS* mutations in a large cohort of mCRC PDXs highlighted the power of PDXs in recapitulating the response to the anti-EGFR antibody cetuximab in patients [188].

Irinotecan, the key component of FOLFIRI combination, is a genotoxic agent that damages the DNA by creating interstrand DNA cross-links and by causing DSBs [191]. Building on this notion, we reasoned that a deeper understanding of the interplay between chemotherapy-induced DNA damage and cell-based activation of the DNA damage response could provide fresh knowledge to dissect the events underlying chemoresistance in mCRC. By detecting the phosphorylation levels of γ-H2AX – a recognized marker of DSBs that participates to DNA repair by mediating the recruitment of other DNA repair proteins around the DSB site – we demonstrated that resistant PDXs showed a less extent of DSB formation upon prolonged treatment with FOLFIRI, compared to sensitive models. This result was integrated by an independent analysis carried out on PDX-matched organoids. In this experimental setting, DSB generation was not analyzed by evaluating the biochemical activation of a DSB sensor but by measuring the physical production of DSBs using the neutral comet assay. Also in this case, similar to that observed in PDXs, organoid models derived from FOLFIRI-resistant PDXs were less prone than FOLFIRI-sensitive PDXs to accumulate DSBs upon irinotecan treatment. Evidence provided by two different approaches in two different, but related, preclinical models strongly support the hypothesis whereby irinotecan sensitivity in mCRC is associated to the exacerbated formation of DSBs after genotoxic treatment. Along the same line, the limited detection of DSBs in resistant tumors suggests that mechanisms are in place to counteract the DNA-damaging activity of irinotecan.

DSBs are typically repaired through the homologous recombination pathway. Hence, differential DSB occurrence in sensitive versus resistant PDXs and organoids could be explained with a different proficiency of the pathway. As HR defects have a synthetic lethal interaction with the inhibition of PARP enzymes, we exploited responsiveness to PARP blockade in selected 3D organoids as a surrogate readout of HR deficiency. We observed that PARP inhibition reduced

cell viability more profoundly in irinotecan-sensitive, DSB-positive organoids than in resistant models with suboptimal DSB formation, corroborating the notion that the inability of cells to repair DSBs by HR pathway plays a pivotal role in mediating chemosensitivity in mCRC. Although the use of PARPis in colorectal cancer has not been extensively explored due to the elevated toxicity in patients [183-185], recent preclinical evidence reported an association between sensitivity to PARPis and defective DNA repair pathways in CRC [186, 198]. This finding strengthens the value of PARPis in selectively distinguishing HR-proficient and HR-deficient tumors and, together with our observations, opens the opportunity to exploit the combinatorial use of PARPis along with irinotecan to increase the depth of response in chemosensitive mCRC. In this scenario, synergistic effects using olaparib and rucaparib in association with SN-38 and irinotecan, respectively, have already been documented in CRC cell lines [178, 180]. Whether the addition of PARPis may sensitize chemorefractory tumors to irinotecan is difficult to anticipate. In principle, if resistance is driven by HR proficiency as we assume, PARPis are not expected to be effective, as demonstrated in *BRCA1/2* wild-type, non-BRCAness breast cancer. However, it is worth noting that replication forks that are stalled due to treatment with topoisomerase I poisons – such as irinotecan – are protected and restarted by PARP trough a mechanism known as fork reversal, which occurs irrespective of HR proficiency [199]. In this scenario, PARP inhibition may be effective in sensitizing to irinotecan by impeding fork reversal, hence in inducing mitotic catastrophe, also in HR-proficient chemorefractory mCRC. For these same reasons, however, the clinical actionability of such a combination may be limited by toxic effects in normal tissues.

To afford our findings with further translational relevance, we decided to assess the feasibility of detecting RAD51, a key HR recombinase, in our FOLFIRI-resistant and sensitive PDXs. We reasoned that the detection of RAD51 in our mCRC models could provide a functional test and deliver a testable biomarker able to predict HR proficiency/chemoresistance, as illustrated for PARPi-resistant breast cancer [195, 196]. Consistent with our assumption that irinotecan-resistant

mCRC enjoys HR functionality, we found that the levels of RAD51 were much higher in FOLFIRI-resistant PDXs compared to the sensitive ones already under basal conditions (in untreated tumors). Moreover, upon treatment all resistant tumors showed an increase of congregation of RAD51 in nuclear foci, indicative of HR pathway activation. These observations suggest that some tumors with intrinsically high RAD51 expression are "primed" for HR-dependent DNA repair and can effectively trigger RAD51 nuclear accumulation for actual HR implementation, thus counteracting the irinotecan genotoxic effect. Our results also demonstrated the usefulness of estimating RAD51 expression as a biomarker of chemoresistance and encourage validation of this approach in independent cohorts of PDXs and human CRC samples.

We found that RAD51-low, irinotecan-sensitive PDXs cycle faster than RAD51-high, irinotecan-resistant tumors. While high proliferative indices have been traditionally correlated with chemosensitivity, the segregation of response with reduced levels of RAD51 may explain, at least partly, the association between marked proliferation and cytotoxicity: whenever highly-proliferating mCRC tumors enter the S-phase, they are repeatedly exposed to a risk of death by irinotecan-triggered DNA damage, which cannot be contrasted because RAD51 levels are low and HR activity is suboptimal. Conversely, slowly-cycling tumors with high RAD51 expression are less prone to irinotecan-mediated cytotoxicity by a two-pronged mechanism: i) the DNA-damaging activity of irinotecan is probabilistically reduced by the fact that a lower number of cells enter S phase; ii) cells in S phase empower RAD51-dependent DNA repair. On the basis of these considerations, we envision that at least an aspect of RAD51-mediated chemoresistance is governed by the different timing of cell-cycle transition

Finally, with the aim to gain further insight into the interplay between HR deficiency and chemosensitivity, we exploited the information obtained from the NGS sequencing of 33 genes belonging to the HR pathway. Genomic profiles of PDXs were unable to distinguish chemoresistant from chemosensitive tumors, with almost all models showing one or more uncharacterized variants of unknown significance in HR genes. Based on published datasets,

HRD genomic signatures appear not be widely represented in CRC, with a prevalence around 2-3% that is much lower than the frequency of FOLFIRI-responsive tumors. Therefore, our results and those from published datasets argue against a genomic basis for the HR deficient/RAD51-low status observed in our sensitive PDXs. Recently gathered data suggest that the abundance of RAD51, and the ensuing modulation of HR proficiency, may be regulated by the differential expression of RAD51 ubiquitin-ligases. If confirmed, this finding would contribute to reconceptualizing the bases of HR deficiency, introducing a new dimension of 'BRCAness' related to regulatory mechanisms of HR proteostasis, such as those mediated by ubiquitin-ligases

Although targeted NGS analysis did not reveal a general segregation of HR genes between FOLFIRI-sensitivie and FOLFIRI-resitant PDX models, specific assessment of the mutational status of the *ATR* gene revealed the presence of heterozygous mutations predominantly clustered within the FOLFIRI-resistant population. The heterozygous nature of the identified mutations suggests a haploinsufficient deleterious phenotype, consistent with the notion that complete loss of function of ATR is incompatible with life. Accordingly, we observed that, after topoisomerase I poisoning, *ATR*-mutant organoids displayed weaker activation of CHK1, a downstream target of ATR, compared to *ATR* wild-type models. We also found that the subset of organoids harboring *ATR* mutations showed increased sensitivity to ATR blockade, whereas *ATR* wild-type organoids were overall more refractory to the action of the ATR inhibitors. This evidence is in line with the finding that ATR hypomorphic protein variants are unable to repair stalled replication forks [200]. In this context, to avoid mitotic catastrophe, cells prematurely engage RAD51, which in turns protects and restarts fork progression trough fork reversal [201]. Hence, cells with *ATR* hypomorphic mutations are "addicted" to RAD51 to progress through the cell cycle. Intriguingly, RAD51 protein abundance is positively regulated by a proficient ATR-CHK1 pathway [197]. This means that cells with hypomorphic *ATR* mutations need to rely on smaller amounts of RAD51 to engender fork reversal and survive, and it is tempting to speculate that pharmacologic blockade of ATR precipitates cell death more markedly in tumors in which *ATR* mutations lead

to reduced RAD51 availability. It is also tempting to speculate that RAD51 inhibitors may synergize with ATR inhibitors in regressing ATR mutant chemorefractory tumors.

Collectively, our data provide preclinical evidence of the contribution of HR in mediating chemotherapy responsiveness in mCRC, putting forward the value of RAD51 as functional biomarker of HR proficiency and chemoresistance. Moreover, we have begun to elucidate the role of *ATR* mutations in chemorefractory tumors; although further experimentation is needed, we suggest a role for *ATR* mutations as negative and positive predictors of response to FOLFIRI and ATR inhibitors, respectively.

MATERIALS AND METHODS

Specimen collection

Tumor samples (liver metastasis and primary tumors) were derived from patients subjected to surgery at Candiolo Cancer Institute (Candiolo, Italy), Mauriziano Umberto I Hospital (Torino, Italy), and San Giovanni Battista (Torino, Italy). All patients provided informed consent. Tumor specimens were maintained in preservation solution (IGL-1) at 4°C and implanted in mice within 24 hours. The study was conducted under the approval of the Review Boards of the Institutions.

Patient-derived xenografts and *in vivo* treatments

Tumor implantation and expansion were performed in 6-week-old male and female NOD/SCID (nonobese diabetic/severe combined immunodeficient) mice as previously described [188]. Once tumors reached an average volume of ~ 400 mm^3, mice were randomized into treatment arms, with n = 5-6 per group, and were treated with the modalities indicated in the figures. Irinotecan (Carbosynth) was administrated twice weekly (25 mg/Kg) in combination with 5-fluorouracil (Selleckchem) (100 mg/Kg) by intraperitoneal injection. Tumor size was evaluated once weekly by caliper measurements, and the approximate volume of the mass was calculated using the formula $4/3\pi\cdot(d/2)^2\cdot D/2$, where d and D are the minor tumor axis and the major tumor axis, respectively. An endpoint of 3 and 6 weeks of treatment was set for each group of arms. Operators were blinded during measurements. *In vivo* procedures and related biobanking data were managed using the Laboratory Assistant Suite (ref). Animal procedures were approved by the Italian Ministry of Health (authorization 806/2016-PR).

Organoids isolation and culture maintenance

Organoids were generated from PDXs. Tumors were cut in a petri dish, washed in Dulbecco's Phosphate Buffered Saline (PBS) (Sigma Aldrich), minced and transferred to 15 ml tube (Falcon) with PBS (Sigma Aldrich), before centrifugation at 900 rpm at 4°C for 5 minutes. Pellet was resuspended in Growth Factor Reduced Matrigel® (Corning) and dispensed in pre-warmed 12-well plate. Organoids were incubated at 37°C in 5% CO_2 for 20 minutes before adding the Dulbecco's Modified Eagle's Medium Nutrient Mixture F-12 Ham (DMEM/F12) medium (Sigma-Aldrich), containing 100 U/mL penicillin-100 µg/mL streptomycin, 200 mM L-glutamine solution, B27 supplement (Invitrogen), N2 supplement (Invitrogen), 1.25 mM N-acetyl-cysteine (Sigma Aldrich), and 20 ng/mL EGF. Organoids were sub-cultured once a week by mechanical disruption.

Immunohistochemical analyses

Tumors were formalin-fixed, paraffin-embedded, and subjected to hematoxylin-and-eosin or immunoperoxidase staining with the following antibodies: rabbit anti-pH2A.X (Ser139) (Cell Signaling Technology #9718S, 1:200), mouse anti-RAD51 (Abcam ab213, 1:500), rabbit anti-Cyclin D1 (Cell Signaling Technology #55506, 1:200), rabbit anti-Cyclin A2 (Abcam ab32386, 1:500), rabbit anti-Cyclin B1 (Abcam ab32053, 1:500). After incubation with secondary antibodies, immunoreactivities were revealed by incubation in DAB chromogen (Dako). Images were captured with the Leica LAS EZ software using a Leica DM LB microscope. Morphometric quantitation was performed by ImageJ software using spectral image segmentation. Software outputs were manually verified by visual inspection of digital images scored through immunohistochemistry as the average of 10 optical fields (40X) randomly chosen from each tumor.

Neutral comet assays

Neutral comet assays were performed using a Trevigen CometAssay® Kit to measure DNA double-strand breaks (DSBs) in response to SN-38 treatment. Briefly, after 4 hours of treatment cells were washed with ice-cold PBS (Sigma Aldrich), harvested, and centrifuged at 1200 rpm at 4°C for 5 minutes. Supernatants were removed, cells were dissociated to single cell and combined with low-melting agarose 1:10 before being spread onto comet slides (Trevigen®). Afterwards, cells were lysed with lysis solution O/N at 4°C. The day after, electrophoresis was performed applying a current of 21 V at 4°C for 45 minutes. Cells were fixed with 70% ethanol, dried and stained with SYBR Green I (Thermo Fisher Scientific) at 1:10000 dilution. Images were acquired using an Leica DMI4000 B microscope equipped with a DFC350 FX camera (Leica). Comet assay quantification was made using imageJ software, comparing mean comet circularity variation upon treatment in at least 50 images/treatment arm, considering a range from 0 to 1 indicating increasing circularity (1= perfect circle).

Biological assays

For cell viability assays, organoids were harvested on ice, washed with ice-cold PBS (Sigma Aldrich), dissociated to single cell using trypsin (Sigma Aldrich) and resuspended in growth medium containing 2% Cultrex growth factor reduced BME type2 (Amsbio). A white, clear bottom 96-well plates (Corning) were coated with 10 µL BME before adding 5000 cells in 100 µL of medium per well. Organoids were let to growth for 5-7 days, then 8 concentrations of ceralasertib, berzosertib, olaparib and niraparib (all Selleckchem) as well as DMSO controls were added in triplicate. Cells were treated with the reported drugs diluted in 2% BME/growth medium for 7 days. Viable cells were measured by ATP content (CellTiter-Glo Reagent, Promega) and luminescence was read on Glomax Discover (Promega). Data were analyzed using GraphPad Prism 8.

Western blot analyses

Before biochemical analysis, organoids were grown in their respective media devoid of drugs or treated as indicated in figure legends.

Total cellular proteins were extracted by lysing cells in boiling Laemmli buffer (1% SDS, 50 mM Tris-HCl [pH 7.5], 150 mM NaCl). Samples were boiled at 95°C for 10 minutes and sonicated and amounts of proteins were normalized with the BCA Protein Assay Reagent Kit (Thermo Scientific). Total proteins were electrophoresed on precasted SDS-polyacrylamide gels (Invitrogen) and transferred onto nitrocellulose membranes (BioRad). Nitrocellulose-bound antibodies were detected by the enhanced chemiluminescence system (Promega). The following primary antibodies were used: rabbit anti-phospho-CHK1 (Ser345) (Cell Signaling Technology #2348, 1:1000), mouse anti-CHK1 (Santa Cruz Biotechnology (G4) sc-8408, 1:200:), mouse anti-Vinculin (Sigma Aldrich, 1:2500).

Genomic analyses

The exonic sequence of 44 HR genes was targeted with a TWIST Bioscience custom capture kit.

Paired end sequencing (2x100) of the obtained fragments was performed on standard Illumina sequencers, aiming at an average depth of 1000X (942.3 was the average depth obtained over all targeted regions for all samples).

Standard QC of the obtained reads was performed with fastqc (version 0.11.7) - variant calls were done following GATK best practices (version 4.1.4.0, bwa version 0.7.17, samtools version 1.9), using Mutect2 in the unpaired mode since the matched germline DNA was not available. To filter possible technical artifacts and germline mutations we used the sets of variants made available by Broad (Panel of Normal and Gnomad dataset). Furthermore, to apply filters specific to our

sequencing protocol, we filtered out the mutations that were reported as possible artifacts by the calling procedure performed by the sequencing vendor.

The only exception to the default pipeline was filtering reads that could have been derived from the xenograft tissue itself, i.e. from the mouse genome, using xenome (version 1.0.0, mouse genome version mm10) prior to alignment to the human genome (hg38).

We also tried to consider the predicted effects of variants on protein function (with VEP version 94.5) and their allelic frequencies, to focus only on the clonal and most functionally relevant variants, to find enrichments in irinotecan sensitive vs resistant models. Since statistical significance was never reached with these progressive filtering (AF > different thresholds, high to modifier variant impact predicted by VEP) for genes different than ATR, in the oncoprint (ComplexHeatmap, version 2.6.2) we included all the non-synonymous mutations.

Statistical analysis

Statistical analyses were performed with MS Excel and Prism GraphPad 8. For cell viability assays, IC_{50} was calculated by non-linear regression, after logarithmic transformation. For all test, P value were calculated using two-tailed Student's t or two-way ANOVA and statical significance was set at $P < 0.05$. Data are showed as mean ± SD with n = 3.

REFERENCES

1. WATSON, J.D. and F.H. CRICK, *Molecular structure of nucleic acids; a structure for deoxyribose nucleic acid.* Nature, 1953. **171**(4356): p. 737-8.
2. Lindahl, T. and D.E. Barnes, *Repair of endogenous DNA damage.* Cold Spring Harb Symp Quant Biol, 2000. **65**: p. 127-33.
3. Friedberg, E.C., *A brief history of the DNA repair field.* Cell Res, 2008. **18**(1): p. 3-7.
4. Hoeijmakers, J.H., *DNA damage, aging, and cancer.* N Engl J Med, 2009. **361**(15): p. 1475-85.
5. Lindahl, T., *Instability and decay of the primary structure of DNA.* Nature, 1993. **362**(6422): p. 709-15.
6. Jackson, S.P. and J. Bartek, *The DNA-damage response in human biology and disease.* Nature, 2009. **461**(7267): p. 1071-8.
7. Branzei, D. and M. Foiani, *Regulation of DNA repair throughout the cell cycle.* Nat Rev Mol Cell Biol, 2008. **9**(4): p. 297-308.
8. Hanahan, D. and R.A. Weinberg, *Hallmarks of cancer: the next generation.* Cell, 2011. **144**(5): p. 646-74.
9. Iyama, T. and D.M. Wilson, *DNA repair mechanisms in dividing and non-dividing cells.* DNA Repair (Amst), 2013. **12**(8): p. 620-36.
10. Larrea, A.A., S.A. Lujan, and T.A. Kunkel, *SnapShot: DNA mismatch repair.* Cell, 2010. **141**(4): p. 730.e1.
11. Jiricny, J., *The multifaceted mismatch-repair system.* Nat Rev Mol Cell Biol, 2006. **7**(5): p. 335-46.
12. Drummond, J.T., et al., *Isolation of an hMSH2-p160 heterodimer that restores DNA mismatch repair to tumor cells.* Science, 1995. **268**(5219): p. 1909-12.
13. Acharya, S., et al., *hMSH2 forms specific mispair-binding complexes with hMSH3 and hMSH6.* Proc Natl Acad Sci U S A, 1996. **93**(24): p. 13629-34.
14. Caldecott, K.W., *Single-strand break repair and genetic disease.* Nat Rev Genet, 2008. **9**(8): p. 619-31.
15. Caldecott, K.W., *Protein ADP-ribosylation and the cellular response to DNA strand breaks.* DNA Repair (Amst), 2014. **19**: p. 108-13.
16. Caldecott, K.W., *DNA single-strand break repair.* Exp Cell Res, 2014. **329**(1): p. 2-8.
17. Sobol, R.W., et al., *The lyase activity of the DNA repair protein beta-polymerase protects from DNA-damage-induced cytotoxicity.* Nature, 2000. **405**(6788): p. 807-10.
18. Symington, L.S. and J. Gautier, *Double-strand break end resection and repair pathway choice.* Annu Rev Genet, 2011. **45**: p. 247-71.
19. Maréchal, A. and L. Zou, *DNA damage sensing by the ATM and ATR kinases.* Cold Spring Harb Perspect Biol, 2013. **5**(9).
20. Blackford, A.N. and S.P. Jackson, *ATM, ATR, and DNA-PK: The Trinity at the Heart of the DNA Damage Response.* Mol Cell, 2017. **66**(6): p. 801-817.
21. Falck, J., et al., *The ATM-Chk2-Cdc25A checkpoint pathway guards against radioresistant DNA synthesis.* Nature, 2001. **410**(6830): p. 842-7.
22. Chehab, N.H., et al., *Chk2/hCds1 functions as a DNA damage checkpoint in G(1) by stabilizing p53.* Genes Dev, 2000. **14**(3): p. 278-88.
23. Campisi, J. and F. d'Adda di Fagagna, *Cellular senescence: when bad things happen to good cells.* Nat Rev Mol Cell Biol, 2007. **8**(9): p. 729-40.
24. Zannini, L., D. Delia, and G. Buscemi, *CHK2 kinase in the DNA damage response and beyond.* J Mol Cell Biol, 2014. **6**(6): p. 442-57.
25. Sullivan, M.R. and K.A. Bernstein, *RAD-ical New Insights into RAD51 Regulation.* Genes (Basel), 2018. **9**(12).

26. San Filippo, J., P. Sung, and H. Klein, *Mechanism of eukaryotic homologous recombination.* Annu Rev Biochem, 2008. **77**: p. 229-57.
27. Cimprich, K.A. and D. Cortez, *ATR: an essential regulator of genome integrity.* Nat Rev Mol Cell Biol, 2008. **9**(8): p. 616-27.
28. Zou, L. and S.J. Elledge, *Sensing DNA damage through ATRIP recognition of RPA-ssDNA complexes.* Science, 2003. **300**(5625): p. 1542-8.
29. Symington, L.S., *Role of RAD52 epistasis group genes in homologous recombination and double-strand break repair.* Microbiol Mol Biol Rev, 2002. **66**(4): p. 630-70, table of contents.
30. Scully, R., et al., *DNA double-strand break repair-pathway choice in somatic mammalian cells.* Nat Rev Mol Cell Biol, 2019. **20**(11): p. 698-714.
31. Noordermeer, S.M., et al., *The shieldin complex mediates 53BP1-dependent DNA repair.* Nature, 2018. **560**(7716): p. 117-121.
32. Ahnesorg, P., P. Smith, and S.P. Jackson, *XLF interacts with the XRCC4-DNA ligase IV complex to promote DNA nonhomologous end-joining.* Cell, 2006. **124**(2): p. 301-13.
33. Chang, H.H.Y., et al., *Non-homologous DNA end joining and alternative pathways to double-strand break repair.* Nat Rev Mol Cell Biol, 2017. **18**(8): p. 495-506.
34. Wood, R.D. and S. Doublié, *DNA polymerase θ (POLQ), double-strand break repair, and cancer.* DNA Repair (Amst), 2016. **44**: p. 22-32.
35. Deans, A.J. and S.C. West, *DNA interstrand crosslink repair and cancer.* Nat Rev Cancer, 2011. **11**(7): p. 467-80.
36. Ceccaldi, R., P. Sarangi, and A.D. D'Andrea, *The Fanconi anaemia pathway: new players and new functions.* Nat Rev Mol Cell Biol, 2016. **17**(6): p. 337-49.
37. Rodríguez, A. and A. D'Andrea, *Fanconi anemia pathway.* Curr Biol, 2017. **27**(18): p. R986-R988.
38. Long, D.T., et al., *Mechanism of RAD51-dependent DNA interstrand cross-link repair.* Science, 2011. **333**(6038): p. 84-7.
39. Wang, X., et al., *Involvement of nucleotide excision repair in a recombination-independent and error-prone pathway of DNA interstrand cross-link repair.* Mol Cell Biol, 2001. **21**(3): p. 713-20.
40. Enoiu, M., J. Jiricny, and O.D. Schärer, *Repair of cisplatin-induced DNA interstrand crosslinks by a replication-independent pathway involving transcription-coupled repair and translesion synthesis.* Nucleic Acids Res, 2012. **40**(18): p. 8953-64.
41. Ghosal, G. and J. Chen, *DNA damage tolerance: a double-edged sword guarding the genome.* Transl Cancer Res, 2013. **2**(3): p. 107-129.
42. Goodman, M.F. and R. Woodgate, *Translesion DNA polymerases.* Cold Spring Harb Perspect Biol, 2013. **5**(10): p. a010363.
43. Bienko, M., et al., *Ubiquitin-binding domains in Y-family polymerases regulate translesion synthesis.* Science, 2005. **310**(5755): p. 1821-4.
44. Motegi, A., et al., *Polyubiquitination of proliferating cell nuclear antigen by HLTF and SHPRH prevents genomic instability from stalled replication forks.* Proc Natl Acad Sci U S A, 2008. **105**(34): p. 12411-6.
45. Markowitz, S.D. and M.M. Bertagnolli, *Molecular origins of cancer: Molecular basis of colorectal cancer.* N Engl J Med, 2009. **361**(25): p. 2449-60.
46. Win, A.K., et al., *Colorectal and other cancer risks for carriers and noncarriers from families with a DNA mismatch repair gene mutation: a prospective cohort study.* J Clin Oncol, 2012. **30**(9): p. 958-64.
47. Hampel, H., et al., *Screening for the Lynch syndrome (hereditary nonpolyposis colorectal cancer).* N Engl J Med, 2005. **352**(18): p. 1851-60.
48. Miki, Y., et al., *A strong candidate for the breast and ovarian cancer susceptibility gene BRCA1.* Science, 1994. **266**(5182): p. 66-71.
49. Wooster, R., et al., *Identification of the breast cancer susceptibility gene BRCA2.* Nature, 1995. **378**(6559): p. 789-92.

50. Hoeijmakers, J.H., *Genome maintenance mechanisms for preventing cancer.* Nature, 2001. **411**(6835): p. 366-74.
51. Lehmann, A.R., *The xeroderma pigmentosum group D (XPD) gene: one gene, two functions, three diseases.* Genes Dev, 2001. **15**(1): p. 15-23.
52. Lindahl, T., B. Demple, and P. Robins, *Suicide inactivation of the E. coli O6-methylguanine-DNA methyltransferase.* EMBO J, 1982. **1**(11): p. 1359-63.
53. Hegi, M.E., et al., *MGMT gene silencing and benefit from temozolomide in glioblastoma.* N Engl J Med, 2005. **352**(10): p. 997-1003.
54. Ranson, M., et al., *Lomeguatrib, a potent inhibitor of O6-alkylguanine-DNA-alkyltransferase: phase I safety, pharmacodynamic, and pharmacokinetic trial and evaluation in combination with temozolomide in patients with advanced solid tumors.* Clin Cancer Res, 2006. **12**(5): p. 1577-84.
55. Curtin, N.J., *DNA repair dysregulation from cancer driver to therapeutic target.* Nat Rev Cancer, 2012. **12**(12): p. 801-17.
56. Abbotts, R. and S. Madhusudan, *Human AP endonuclease 1 (APE1): from mechanistic insights to druggable target in cancer.* Cancer Treat Rev, 2010. **36**(5): p. 425-35.
57. Hirai, K., K. Ueda, and O. Hayaishi, *Aberration of poly(adenosine diphosphate-ribose) metabolism in human colon adenomatous polyps and cancers.* Cancer Res, 1983. **43**(7): p. 3441-6.
58. Plumb, J.A., et al., *Reversal of drug resistance in human tumor xenografts by 2'-deoxy-5-azacytidine-induced demethylation of the hMLH1 gene promoter.* Cancer Res, 2000. **60**(21): p. 6039-44.
59. Shinohara, E.T., et al., *DNA-dependent protein kinase is a molecular target for the development of noncytotoxic radiation-sensitizing drugs.* Cancer Res, 2005. **65**(12): p. 4987-92.
60. Zhao, Y., et al., *Preclinical evaluation of a potent novel DNA-dependent protein kinase inhibitor NU7441.* Cancer Res, 2006. **66**(10): p. 5354-62.
61. Munck, J.M., et al., *Chemosensitization of cancer cells by KU-0060648, a dual inhibitor of DNA-PK and PI-3K.* Mol Cancer Ther, 2012. **11**(8): p. 1789-98.
62. DOBZHANSKY, T., *Genetics of natural populations; recombination and variability in populations of Drosophila pseudoobscura.* Genetics, 1946. **31**: p. 269-90.
63. Hartwell, L.H., et al., *Integrating genetic approaches into the discovery of anticancer drugs.* Science, 1997. **278**(5340): p. 1064-8.
64. Bryant, H.E., et al., *Specific killing of BRCA2-deficient tumours with inhibitors of poly(ADP-ribose) polymerase.* Nature, 2005. **434**(7035): p. 913-7.
65. Farmer, H., et al., *Targeting the DNA repair defect in BRCA mutant cells as a therapeutic strategy.* Nature, 2005. **434**(7035): p. 917-21.
66. Kim, G., et al., *FDA Approval Summary: Olaparib Monotherapy in Patients with Deleterious Germline BRCA-Mutated Advanced Ovarian Cancer Treated with Three or More Lines of Chemotherapy.* Clin Cancer Res, 2015. **21**(19): p. 4257-61.
67. Balasubramaniam, S., et al., *FDA Approval Summary: Rucaparib for the Treatment of Patients with Deleterious.* Clin Cancer Res, 2017. **23**(23): p. 7165-7170.
68. González-Martín, A., et al., *Niraparib in Patients with Newly Diagnosed Advanced Ovarian Cancer.* N Engl J Med, 2019. **381**(25): p. 2391-2402.
69. Litton, J.K., et al., *Talazoparib in Patients with Advanced Breast Cancer and a Germline BRCA Mutation.* N Engl J Med, 2018. **379**(8): p. 753-763.
70. Golan, T., et al., *Maintenance Olaparib for Germline.* N Engl J Med, 2019. **381**(4): p. 317-327.
71. de Bono, J., et al., *Olaparib for Metastatic Castration-Resistant Prostate Cancer.* N Engl J Med, 2020. **382**(22): p. 2091-2102.
72. Abida, W., et al., *Rucaparib in Men With Metastatic Castration-Resistant Prostate Cancer Harboring a.* J Clin Oncol, 2020. **38**(32): p. 3763-3772.

73. Curtin, N.J. and C. Szabo, *Poly(ADP-ribose) polymerase inhibition: past, present and future.* Nat Rev Drug Discov, 2020. **19**(10): p. 711-736.
74. Murai, J., et al., *Stereospecific PARP trapping by BMN 673 and comparison with olaparib and rucaparib.* Mol Cancer Ther, 2014. **13**(2): p. 433-43.
75. Coleman, R.L., et al., *Rucaparib maintenance treatment for recurrent ovarian carcinoma after response to platinum therapy (ARIEL3): a randomised, double-blind, placebo-controlled, phase 3 trial.* Lancet, 2017. **390**(10106): p. 1949-1961.
76. Ray-Coquard, I., et al., *Olaparib plus Bevacizumab as First-Line Maintenance in Ovarian Cancer.* N Engl J Med, 2019. **381**(25): p. 2416-2428.
77. Swisher, E.M., et al., *Rucaparib in relapsed, platinum-sensitive high-grade ovarian carcinoma (ARIEL2 Part 1): an international, multicentre, open-label, phase 2 trial.* Lancet Oncol, 2017. **18**(1): p. 75-87.
78. Hodgson, D.R., et al., *Candidate biomarkers of PARP inhibitor sensitivity in ovarian cancer beyond the BRCA genes.* Br J Cancer, 2018. **119**(11): p. 1401-1409.
79. Mateo, J., et al., *DNA-Repair Defects and Olaparib in Metastatic Prostate Cancer.* N Engl J Med, 2015. **373**(18): p. 1697-708.
80. Abida, W., et al., *Non-BRCA DNA Damage Repair Gene Alterations and Response to the PARP Inhibitor Rucaparib in Metastatic Castration-Resistant Prostate Cancer: Analysis From the Phase II TRITON2 Study.* Clin Cancer Res, 2020. **26**(11): p. 2487-2496.
81. Lord, C.J. and A. Ashworth, *BRCAness revisited.* Nat Rev Cancer, 2016. **16**(2): p. 110-20.
82. Tung, N.M., et al., *TBCRC 048: Phase II Study of Olaparib for Metastatic Breast Cancer and Mutations in Homologous Recombination-Related Genes.* J Clin Oncol, 2020. **38**(36): p. 4274-4282.
83. Grellety, T., et al., *Dramatic response to PARP inhibition in a PALB2-mutated breast cancer: moving beyond BRCA.* Ann Oncol, 2020. **31**(6): p. 822-823.
84. Kondrashova, O., et al., *Secondary Somatic Mutations Restoring.* Cancer Discov, 2017. **7**(9): p. 984-998.
85. Shen, J., et al., *ARID1A Deficiency Impairs the DNA Damage Checkpoint and Sensitizes Cells to PARP Inhibitors.* Cancer Discov, 2015. **5**(7): p. 752-67.
86. Parrotta, R., et al., *A Novel BRCA1-Associated Protein-1 Isoform Affects Response of Mesothelioma Cells to Drugs Impairing BRCA1-Mediated DNA Repair.* J Thorac Oncol, 2017. **12**(8): p. 1309-1319.
87. Sulkowski, P.L., et al., *Krebs-cycle-deficient hereditary cancer syndromes are defined by defects in homologous-recombination DNA repair.* Nat Genet, 2018. **50**(8): p. 1086-1092.
88. Sulkowski, P.L., et al., *Oncometabolites suppress DNA repair by disrupting local chromatin signalling.* Nature, 2020. **582**(7813): p. 586-591.
89. Lallo, A., et al., *The Combination of the PARP Inhibitor Olaparib and the WEE1 Inhibitor AZD1775 as a New Therapeutic Option for Small Cell Lung Cancer.* Clin Cancer Res, 2018. **24**(20): p. 5153-5164.
90. Yazinski, S.A., et al., *ATR inhibition disrupts rewired homologous recombination and fork protection pathways in PARP inhibitor-resistant BRCA-deficient cancer cells.* Genes Dev, 2017. **31**(3): p. 318-332.
91. Kim, H., et al., *Targeting the ATR/CHK1 Axis with PARP Inhibition Results in Tumor Regression in.* Clin Cancer Res, 2017. **23**(12): p. 3097-3108.
92. Asim, M., et al., *Synthetic lethality between androgen receptor signalling and the PARP pathway in prostate cancer.* Nat Commun, 2017. **8**(1): p. 374.
93. Li, L., et al., *Androgen receptor inhibitor-induced "BRCAness" and PARP inhibition are synthetically lethal for castration-resistant prostate cancer.* Sci Signal, 2017. **10**(480).

94. Clarke, N., et al., *Olaparib combined with abiraterone in patients with metastatic castration-resistant prostate cancer: a randomised, double-blind, placebo-controlled, phase 2 trial.* Lancet Oncol, 2018. **19**(7): p. 975-986.
95. Hussain, M., et al., *Targeting Androgen Receptor and DNA Repair in Metastatic Castration-Resistant Prostate Cancer: Results From NCI 9012.* J Clin Oncol, 2018. **36**(10): p. 991-999.
96. Mo, W., et al., *mTOR Inhibitors Suppress Homologous Recombination Repair and Synergize with PARP Inhibitors via Regulating SUV39H1 in BRCA-Proficient Triple-Negative Breast Cancer.* Clin Cancer Res, 2016. **22**(7): p. 1699-712.
97. Matulonis, U.A., et al., *Phase I dose escalation study of the PI3kinase pathway inhibitor BKM120 and the oral poly (ADP ribose) polymerase (PARP) inhibitor olaparib for the treatment of high-grade serous ovarian and breast cancer.* Ann Oncol, 2017. **28**(3): p. 512-518.
98. Konstantinopoulos, P.A., et al., *Olaparib and α-specific PI3K inhibitor alpelisib for patients with epithelial ovarian cancer: a dose-escalation and dose-expansion phase 1b trial.* Lancet Oncol, 2019. **20**(4): p. 570-580.
99. Sun, C., et al., *Rational combination therapy with PARP and MEK inhibitors capitalizes on therapeutic liabilities in.* Sci Transl Med, 2017. **9**(392).
100. Liu, J.F., et al., *Combination cediranib and olaparib versus olaparib alone for women with recurrent platinum-sensitive ovarian cancer: a randomised phase 2 study.* Lancet Oncol, 2014. **15**(11): p. 1207-14.
101. Sun, C., et al., *BRD4 Inhibition Is Synthetic Lethal with PARP Inhibitors through the Induction of Homologous Recombination Deficiency.* Cancer Cell, 2018. **33**(3): p. 401-416.e8.
102. Parkes, E.E., et al., *Activation of STING-Dependent Innate Immune Signaling By S-Phase-Specific DNA Damage in Breast Cancer.* J Natl Cancer Inst, 2017. **109**(1).
103. Jiao, S., et al., *PARP Inhibitor Upregulates PD-L1 Expression and Enhances Cancer-Associated Immunosuppression.* Clin Cancer Res, 2017. **23**(14): p. 3711-3720.
104. Lee, J.M., et al., *Safety and Clinical Activity of the Programmed Death-Ligand 1 Inhibitor Durvalumab in Combination With Poly (ADP-Ribose) Polymerase Inhibitor Olaparib or Vascular Endothelial Growth Factor Receptor 1-3 Inhibitor Cediranib in Women's Cancers: A Dose-Escalation, Phase I Study.* J Clin Oncol, 2017. **35**(19): p. 2193-2202.
105. Domchek, S.M., et al., *Olaparib and durvalumab in patients with germline BRCA-mutated metastatic breast cancer (MEDIOLA): an open-label, multicentre, phase 1/2, basket study.* Lancet Oncol, 2020. **21**(9): p. 1155-1164.
106. Shen, J., et al., *PARPi Triggers the STING-Dependent Immune Response and Enhances the Therapeutic Efficacy of Immune Checkpoint Blockade Independent of BRCAness.* Cancer Res, 2019. **79**(2): p. 311-319.
107. Pilié, P.G., et al., *State-of-the-art strategies for targeting the DNA damage response in cancer.* Nat Rev Clin Oncol, 2019. **16**(2): p. 81-104.
108. Welch, S., et al., *UCN-01 in combination with topotecan in patients with advanced recurrent ovarian cancer: a study of the Princess Margaret Hospital Phase II consortium.* Gynecol Oncol, 2007. **106**(2): p. 305-10.
109. Ma, C.X., et al., *A phase II study of UCN-01 in combination with irinotecan in patients with metastatic triple negative breast cancer.* Breast Cancer Res Treat, 2013. **137**(2): p. 483-92.
110. A. L. Ho , J.C.B., J. M. Cleary , G. K. Schwartz , H. A. Burris , P. Oakes F. Agbo , P. N. Barker , A. M. Senderowicz , G. Shapiro, *Phase I, open-label, dose-escalation study of AZD7762 in combination with irinotecan (irino) in patients (pts) with advanced solid tumors*. 2011, *J. Clin. Oncol*.

111. Sausville, E., et al., *Phase I dose-escalation study of AZD7762, a checkpoint kinase inhibitor, in combination with gemcitabine in US patients with advanced solid tumors.* Cancer Chemother Pharmacol, 2014. **73**(3): p. 539-49.
112. Laquente, B., et al., *A phase II study to evaluate LY2603618 in combination with gemcitabine in pancreatic cancer patients.* BMC Cancer, 2017. **17**(1): p. 137.
113. Daud, A.I., et al., *Phase I dose-escalation trial of checkpoint kinase 1 inhibitor MK-8776 as monotherapy and in combination with gemcitabine in patients with advanced solid tumors.* J Clin Oncol, 2015. **33**(9): p. 1060-6.
114. Hong, D.S., et al., *Evaluation of Prexasertib, a Checkpoint Kinase 1 Inhibitor, in a Phase Ib Study of Patients with Squamous Cell Carcinoma.* Clin Cancer Res, 2018. **24**(14): p. 3263-3272.
115. Hirai, H., et al., *Small-molecule inhibition of Wee1 kinase by MK-1775 selectively sensitizes p53-deficient tumor cells to DNA-damaging agents.* Mol Cancer Ther, 2009. **8**(11): p. 2992-3000.
116. Bridges, K.A., et al., *MK-1775, a novel Wee1 kinase inhibitor, radiosensitizes p53-defective human tumor cells.* Clin Cancer Res, 2011. **17**(17): p. 5638-48.
117. Leijen, S., et al., *Phase I Study Evaluating WEE1 Inhibitor AZD1775 As Monotherapy and in Combination With Gemcitabine, Cisplatin, or Carboplatin in Patients With Advanced Solid Tumors.* J Clin Oncol, 2016. **34**(36): p. 4371-4380.
118. Ceccaldi, R., et al., *Homologous-recombination-deficient tumours are dependent on Polθ-mediated repair.* Nature, 2015. **518**(7538): p. 258-62.
119. Siegel, R.L., K.D. Miller, and A. Jemal, *Cancer statistics, 2020.* CA Cancer J Clin, 2020. **70**(1): p. 7-30.
120. Ferlay, J., et al., *Cancer incidence and mortality patterns in Europe: Estimates for 40 countries and 25 major cancers in 2018.* Eur J Cancer, 2018. **103**: p. 356-387.
121. Advani, S. and S. Kopetz, *Ongoing and future directions in the management of metastatic colorectal cancer: Update on clinical trials.* J Surg Oncol, 2019. **119**(5): p. 642-652.
122. Dekker, E., et al., *Colorectal cancer.* Lancet, 2019. **394**(10207): p. 1467-1480.
123. Vogelstein, B., et al., *Genetic alterations during colorectal-tumor development.* N Engl J Med, 1988. **319**(9): p. 525-32.
124. Boland, C.R., et al., *A National Cancer Institute Workshop on Microsatellite Instability for cancer detection and familial predisposition: development of international criteria for the determination of microsatellite instability in colorectal cancer.* Cancer Res, 1998. **58**(22): p. 5248-57.
125. Weisenberger, D.J., et al., *CpG island methylator phenotype underlies sporadic microsatellite instability and is tightly associated with BRAF mutation in colorectal cancer.* Nat Genet, 2006. **38**(7): p. 787-93.
126. Funkhouser, W.K., et al., *Relevance, pathogenesis, and testing algorithm for mismatch repair-defective colorectal carcinomas: a report of the association for molecular pathology.* J Mol Diagn, 2012. **14**(2): p. 91-103.
127. Tol, J., I.D. Nagtegaal, and C.J. Punt, *BRAF mutation in metastatic colorectal cancer.* N Engl J Med, 2009. **361**(1): p. 98-9.
128. Syngal, S., et al., *ACG clinical guideline: Genetic testing and management of hereditary gastrointestinal cancer syndromes.* Am J Gastroenterol, 2015. **110**(2): p. 223-62; quiz 263.
129. Lynch, H.T., et al., *Milestones of Lynch syndrome: 1895-2015.* Nat Rev Cancer, 2015. **15**(3): p. 181-94.
130. Kuipers, E.J., et al., *Colorectal cancer.* Nat Rev Dis Primers, 2015. **1**: p. 15065.
131. Avolio, M. and L. Trusolino, *Rational Treatment of Metastatic Colorectal Cancer: A Reverse Tale of Men, Mice, and Culture Dishes.* Cancer Discov, 2021. **11**(7): p. 1644-1660.

132. Douillard, J.Y., et al., *Randomized, phase III trial of panitumumab with infusional fluorouracil, leucovorin, and oxaliplatin (FOLFOX4) versus FOLFOX4 alone as first-line treatment in patients with previously untreated metastatic colorectal cancer: the PRIME study.* J Clin Oncol, 2010. **28**(31): p. 4697-705.
133. Hurwitz, H., et al., *Bevacizumab plus irinotecan, fluorouracil, and leucovorin for metastatic colorectal cancer.* N Engl J Med, 2004. **350**(23): p. 2335-42.
134. Saltz, L.B., et al., *Bevacizumab in combination with oxaliplatin-based chemotherapy as first-line therapy in metastatic colorectal cancer: a randomized phase III study.* J Clin Oncol, 2008. **26**(12): p. 2013-9.
135. Van Cutsem, E., et al., *Addition of aflibercept to fluorouracil, leucovorin, and irinotecan improves survival in a phase III randomized trial in patients with metastatic colorectal cancer previously treated with an oxaliplatin-based regimen.* J Clin Oncol, 2012. **30**(28): p. 3499-506.
136. Tabernero, J., et al., *Ramucirumab versus placebo in combination with second-line FOLFIRI in patients with metastatic colorectal carcinoma that progressed during or after first-line therapy with bevacizumab, oxaliplatin, and a fluoropyrimidine (RAISE): a randomised, double-blind, multicentre, phase 3 study.* Lancet Oncol, 2015. **16**(5): p. 499-508.
137. Grothey, A., et al., *Regorafenib monotherapy for previously treated metastatic colorectal cancer (CORRECT): an international, multicentre, randomised, placebo-controlled, phase 3 trial.* Lancet, 2013. **381**(9863): p. 303-12.
138. Sartore-Bianchi, A., et al., *Dual-targeted therapy with trastuzumab and lapatinib in treatment-refractory, KRAS codon 12/13 wild-type, HER2-positive metastatic colorectal cancer (HERACLES): a proof-of-concept, multicentre, open-label, phase 2 trial.* Lancet Oncol, 2016. **17**(6): p. 738-746.
139. Meric-Bernstam, F., et al., *Pertuzumab plus trastuzumab for HER2-amplified metastatic colorectal cancer (MyPathway): an updated report from a multicentre, open-label, phase 2a, multiple basket study.* Lancet Oncol, 2019. **20**(4): p. 518-530.
140. Sartore-Bianchi, A., et al., *Sensitivity to Entrectinib Associated With a Novel LMNA-NTRK1 Gene Fusion in Metastatic Colorectal Cancer.* J Natl Cancer Inst, 2016. **108**(1).
141. Gozgit, J.M., et al., *RET fusions observed in lung and colorectal cancers are sensitive to ponatinib.* Oncotarget, 2018. **9**(51): p. 29654-29664.
142. De Roock, W., et al., *KRAS, BRAF, PIK3CA, and PTEN mutations: implications for targeted therapies in metastatic colorectal cancer.* Lancet Oncol, 2011. **12**(6): p. 594-603.
143. Van Cutsem, E., et al., *ESMO consensus guidelines for the management of patients with metastatic colorectal cancer.* Ann Oncol, 2016. **27**(8): p. 1386-422.
144. Ahronian, L.G., et al., *Clinical Acquired Resistance to RAF Inhibitor Combinations in BRAF-Mutant Colorectal Cancer through MAPK Pathway Alterations.* Cancer Discov, 2015. **5**(4): p. 358-67.
145. Prahallad, A., et al., *Unresponsiveness of colon cancer to BRAF(V600E) inhibition through feedback activation of EGFR.* Nature, 2012. **483**(7387): p. 100-3.
146. Kopetz, S., et al., *Encorafenib, Binimetinib, and Cetuximab in.* N Engl J Med, 2019. **381**(17): p. 1632-1643.
147. de Gramont, A., et al., *Leucovorin and fluorouracil with or without oxaliplatin as first-line treatment in advanced colorectal cancer.* J Clin Oncol, 2000. **18**(16): p. 2938-47.
148. Douillard, J.Y., et al., *Irinotecan combined with fluorouracil compared with fluorouracil alone as first-line treatment for metastatic colorectal cancer: a multicentre randomised trial.* Lancet, 2000. **355**(9209): p. 1041-7.
149. Falcone, A., et al., *Phase III trial of infusional fluorouracil, leucovorin, oxaliplatin, and irinotecan (FOLFOXIRI) compared with infusional fluorouracil, leucovorin, and irinotecan (FOLFIRI) as first-line treatment for metastatic colorectal cancer: the Gruppo Oncologico Nord Ovest.* J Clin Oncol, 2007. **25**(13): p. 1670-6.

150. Arkenau, H.T., et al., *Efficacy of oxaliplatin plus capecitabine or infusional fluorouracil/leucovorin in patients with metastatic colorectal cancer: a pooled analysis of randomized trials.* J Clin Oncol, 2008. **26**(36): p. 5910-7.
151. Köhne, C.H., et al., *Irinotecan combined with infusional 5-fluorouracil/folinic acid or capecitabine plus celecoxib or placebo in the first-line treatment of patients with metastatic colorectal cancer. EORTC study 40015.* Ann Oncol, 2008. **19**(5): p. 920-6.
152. Xu, R.H., et al., *Modified XELIRI (capecitabine plus irinotecan) versus FOLFIRI (leucovorin, fluorouracil, and irinotecan), both either with or without bevacizumab, as second-line therapy for metastatic colorectal cancer (AXEPT): a multicentre, open-label, randomised, non-inferiority, phase 3 trial.* Lancet Oncol, 2018. **19**(5): p. 660-671.
153. Edler, D., et al., *Thymidylate synthase expression in colorectal cancer: a prognostic and predictive marker of benefit from adjuvant fluorouracil-based chemotherapy.* J Clin Oncol, 2002. **20**(7): p. 1721-8.
154. Kornmann, M., et al., *Thymidylate synthase and dihydropyrimidine dehydrogenase mRNA expression levels: predictors for survival in colorectal cancer patients receiving adjuvant 5-fluorouracil.* Clin Cancer Res, 2003. **9**(11): p. 4116-24.
155. Salonga, D., et al., *Colorectal tumors responding to 5-fluorouracil have low gene expression levels of dihydropyrimidine dehydrogenase, thymidylate synthase, and thymidine phosphorylase.* Clin Cancer Res, 2000. **6**(4): p. 1322-7.
156. Soong, R., et al., *Prognostic significance of thymidylate synthase, dihydropyrimidine dehydrogenase and thymidine phosphorylase protein expression in colorectal cancer patients treated with or without 5-fluorouracil-based chemotherapy.* Ann Oncol, 2008. **19**(5): p. 915-9.
157. Braun, M.S., et al., *Predictive biomarkers of chemotherapy efficacy in colorectal cancer: results from the UK MRC FOCUS trial.* J Clin Oncol, 2008. **26**(16): p. 2690-8.
158. Vallböhmer, D., et al., *DPD is a molecular determinant of capecitabine efficacy in colorectal cancer.* Int J Oncol, 2007. **31**(2): p. 413-8.
159. Koopman, M., et al., *Predictive and prognostic markers for the outcome of chemotherapy in advanced colorectal cancer, a retrospective analysis of the phase III randomised CAIRO study.* Eur J Cancer, 2009. **45**(11): p. 1999-2006.
160. Deenen, M.J., et al., *Relationship between single nucleotide polymorphisms and haplotypes in DPYD and toxicity and efficacy of capecitabine in advanced colorectal cancer.* Clin Cancer Res, 2011. **17**(10): p. 3455-68.
161. Meulendijks, D., et al., *Clinical relevance of DPYD variants c.1679T>G, c.1236G>A/HapB3, and c.1601G>A as predictors of severe fluoropyrimidine-associated toxicity: a systematic review and meta-analysis of individual patient data.* Lancet Oncol, 2015. **16**(16): p. 1639-50.
162. Henricks, L.M., et al., *DPYD genotype-guided dose individualisation of fluoropyrimidine therapy in patients with cancer: a prospective safety analysis.* Lancet Oncol, 2018. **19**(11): p. 1459-1467.
163. Cheng, L., et al., *UGT1A1*6 polymorphisms are correlated with irinotecan-induced toxicity: a system review and meta-analysis in Asians.* Cancer Chemother Pharmacol, 2014. **73**(3): p. 551-60.
164. Tejpar, S., et al., *Clinical and pharmacogenetic determinants of 5-fluorouracyl/leucovorin/irinotecan toxicity: Results of the PETACC-3 trial.* Eur J Cancer, 2018. **99**: p. 66-77.
165. Shirota, Y., et al., *ERCC1 and thymidylate synthase mRNA levels predict survival for colorectal cancer patients receiving combination oxaliplatin and fluorouracil chemotherapy.* J Clin Oncol, 2001. **19**(23): p. 4298-304.
166. Viguier, J., et al., *ERCC1 codon 118 polymorphism is a predictive factor for the tumor response to oxaliplatin/5-fluorouracil combination chemotherapy in patients with advanced colorectal cancer.* Clin Cancer Res, 2005. **11**(17): p. 6212-7.

167. Parikh, A.R., et al., *MAVERICC, a Randomized, Biomarker-stratified, Phase II Study of mFOLFOX6-Bevacizumab versus FOLFIRI-Bevacizumab as First-line Chemotherapy in Metastatic Colorectal Cancer.* Clin Cancer Res, 2019. **25**(10): p. 2988-2995.
168. Formica, V., et al., *Biological and predictive role of ERCC1 polymorphisms in cancer.* Crit Rev Oncol Hematol, 2017. **111**: p. 133-143.
169. Germano, G., et al., *Inactivation of DNA repair triggers neoantigen generation and impairs tumour growth.* Nature, 2017. **552**(7683): p. 116-120.
170. Le, D.T., et al., *PD-1 Blockade in Tumors with Mismatch-Repair Deficiency.* N Engl J Med, 2015. **372**(26): p. 2509-20.
171. Overman, M.J., et al., *Nivolumab in patients with metastatic DNA mismatch repair-deficient or microsatellite instability-high colorectal cancer (CheckMate 142): an open-label, multicentre, phase 2 study.* Lancet Oncol, 2017. **18**(9): p. 1182-1191.
172. Le, D.T., et al., *Mismatch repair deficiency predicts response of solid tumors to PD-1 blockade.* Science, 2017. **357**(6349): p. 409-413.
173. Soyano, A.E., C. Baldeo, and P.M. Kasi, *BRCA Mutation and Its Association With Colorectal Cancer.* Clin Colorectal Cancer, 2018. **17**(4): p. e647-e650.
174. Knijnenburg, T.A., et al., *Genomic and Molecular Landscape of DNA Damage Repair Deficiency across The Cancer Genome Atlas.* Cell Rep, 2018. **23**(1): p. 239-254.e6.
175. McAndrew, E.N., C.C. Lepage, and K.J. McManus, *The synthetic lethal killing of RAD54B-deficient colorectal cancer cells by PARP1 inhibition is enhanced with SOD1 inhibition.* Oncotarget, 2016. **7**(52): p. 87417-87430.
176. Wang, C., et al., *ATM-Deficient Colorectal Cancer Cells Are Sensitive to the PARP Inhibitor Olaparib.* Transl Oncol, 2017. **10**(2): p. 190-196.
177. Xu, K., et al., *Combined olaparib and oxaliplatin inhibits tumor proliferation and induces G2/M arrest and γ-H2AX foci formation in colorectal cancer.* Onco Targets Ther, 2015. **8**: p. 3047-54.
178. Tahara, M., et al., *The use of Olaparib (AZD2281) potentiates SN-38 cytotoxicity in colon cancer cells by indirect inhibition of Rad51-mediated repair of DNA double-strand breaks.* Mol Cancer Ther, 2014. **13**(5): p. 1170-80.
179. Genther Williams, S.M., et al., *Treatment with the PARP inhibitor, niraparib, sensitizes colorectal cancer cell lines to irinotecan regardless of MSI/MSS status.* Cancer Cell Int, 2015. **15**(1): p. 14.
180. Augustine, T., et al., *Sensitization of colorectal cancer to irinotecan therapy by PARP inhibitor rucaparib.* Invest New Drugs, 2019. **37**(5): p. 948-960.
181. Greene, J., et al., *The novel ATM inhibitor (AZ31) enhances antitumor activity in patient derived xenografts that are resistant to irinotecan monotherapy.* Oncotarget, 2017. **8**(67): p. 110904-110913.
182. Dietlein, F., et al., *A Synergistic Interaction between Chk1- and MK2 Inhibitors in KRAS-Mutant Cancer.* Cell, 2015. **162**(1): p. 146-59.
183. Leichman, L., et al., *Phase II Study of Olaparib (AZD-2281) After Standard Systemic Therapies for Disseminated Colorectal Cancer.* Oncologist, 2016. **21**(2): p. 172-7.
184. Gorbunova, V., et al., *A phase 2 randomised study of veliparib plus FOLFIRI±bevacizumab versus placebo plus FOLFIRI±bevacizumab in metastatic colorectal cancer.* Br J Cancer, 2019. **120**(2): p. 183-189.
185. Pishvaian, M.J., et al., *A phase 2 study of the PARP inhibitor veliparib plus temozolomide in patients with heavily pretreated metastatic colorectal cancer.* Cancer, 2018. **124**(11): p. 2337-2346.
186. Arena, S., et al., *A Subset of Colorectal Cancers with Cross-Sensitivity to Olaparib and Oxaliplatin.* Clin Cancer Res, 2020. **26**(6): p. 1372-1384.
187. Arai, H., et al., *The Landscape of Alterations in DNA Damage Response Pathways in Colorectal Cancer.* Clin Cancer Res, 2021. **27**(11): p. 3234-3242.

188. Bertotti, A., et al., *A molecularly annotated platform of patient-derived xenografts ("xenopatients") identifies HER2 as an effective therapeutic target in cetuximab-resistant colorectal cancer.* Cancer Discov, 2011. **1**(6): p. 508-23.
189. Bertotti, A., et al., *The genomic landscape of response to EGFR blockade in colorectal cancer.* Nature, 2015. **526**(7572): p. 263-7.
190. Colucci, G., et al., *Phase III randomized trial of FOLFIRI versus FOLFOX4 in the treatment of advanced colorectal cancer: a multicenter study of the Gruppo Oncologico Dell'Italia Meridionale.* J Clin Oncol, 2005. **23**(22): p. 4866-75.
191. Pommier, Y., *Topoisomerase I inhibitors: camptothecins and beyond.* Nat Rev Cancer, 2006. **6**(10): p. 789-802.
192. Redon, C.E., et al., *Histone gammaH2AX and poly(ADP-ribose) as clinical pharmacodynamic biomarkers.* Clin Cancer Res, 2010. **16**(18): p. 4532-42.
193. Sharma, A., K. Singh, and A. Almasan, *Histone H2AX phosphorylation: a marker for DNA damage.* Methods Mol Biol, 2012. **920**: p. 613-26.
194. Olive, P.L. and J.P. Banáth, *The comet assay: a method to measure DNA damage in individual cells.* Nat Protoc, 2006. **1**(1): p. 23-9.
195. Cruz, C., et al., *RAD51 foci as a functional biomarker of homologous recombination repair and PARP inhibitor resistance in germline BRCA-mutated breast cancer.* Ann Oncol, 2018. **29**(5): p. 1203-1210.
196. Castroviejo-Bermejo, M., et al., *A RAD51 assay feasible in routine tumor samples calls PARP inhibitor response beyond BRCA mutation.* EMBO Mol Med, 2018. **10**(12).
197. Marzio, A., et al., *The F-Box Domain-Dependent Activity of EMI1 Regulates PARPi Sensitivity in Triple-Negative Breast Cancers.* Mol Cell, 2019. **73**(2): p. 224-237.e6.
198. Smeby, J., et al., *Molecular correlates of sensitivity to PARP inhibition beyond homologous recombination deficiency in pre-clinical models of colorectal cancer point to wild-type TP53 activity.* EBioMedicine, 2020. **59**: p. 102923.
199. Ray Chaudhuri, A., et al., *Topoisomerase I poisoning results in PARP-mediated replication fork reversal.* Nat Struct Mol Biol, 2012. **19**(4): p. 417-23.
200. Saldivar, J.C., D. Cortez, and K.A. Cimprich, *The essential kinase ATR: ensuring faithful duplication of a challenging genome.* Nat Rev Mol Cell Biol, 2017. **18**(10): p. 622-636.
201. Zellweger, R., et al., *Rad51-mediated replication fork reversal is a global response to genotoxic treatments in human cells.* J Cell Biol, 2015. **208**(5): p. 563-79.